SEDIMENTOLOGY the journal of the International Association of Sedimentologists

Sedimentology (2021) **68**, 2887–2917 doi: 10.1111/sed.12876

Spatial variation in the sedimentary architecture of a dryland fluvial system

CHARLOTTE L. PRIDDY and STUART M. CLARKE
Basin Dynamics Research Group, School of Geography, Geology and the Environment, Keele University, Keele, Staffordshire, ST5 5BG, UK (E-mail: c.priddy@keele.ac.uk)

Associate Editor – Christopher Fielding

ABSTRACT

Ancient dryland terminal fluvial systems are often recognized within the rock record for having a progressive downstream decrease in the size and amalgamation of channel elements and systematic downstream increase in sheet and overbank elements, alongside the downstream decrease in grain size that is displayed by most fluvial systems. The spatial distribution and downstream trends displayed by the fluvial sediments of the Lower Jurassic Kayenta Formation of south-western USA, have been examined quantitatively. The results indicate many trends that are similar to those of a dryland terminal fluvial system, including; a lack of confinement of the fluvial system, a downstream decrease in channel and sheet element amalgamation and width-to-thickness ratios, a downstream decrease in grain size, albeit very small, and an increase in the percentage of overbank elements downstream. However, the study highlights several downstream relationships that are atypical. While some of these relationships may be the result of external factors inherent in this study, others, including the thicknesses of channel-fill and sheet elements that display no significant relationships to distance downstream, and channel-fill elements that display no significant variation in average grain size with distance downstream, may be a consequence of fluvial interaction with a competing and coeval aeolian system. This work demonstrates the inherent complexity in arid dryland fluvial systems and the downstream architectural and compositional relationships that they depict. Consequently, models for fluvial style may provide only a first-order approximation for downstream trends in dryland systems, because the controlling factors upon these systems are inherently difficult to unravel, and the sedimentary detail is strongly dependent upon external setting and internal complexity. Consequently, a generalized model may not always be applicable to these systems.

Keywords Aeolian, distributive fluvial systems, dryland, ephemeral–fluvial, Kayenta Formation.

INTRODUCTION

Fluvial systems are typically classified by hydrological regime (for example, ephemeral versus perennial), by planform morphology (for example, braided or meandering) and by prevailing climatic regime (for example, arid, semi-arid, sub-humid, per-humid) (Colombera *et al.*, 2013; Colombera & Mountney, 2019). Although classification of fluvial style using these terms is typically a factor of the scale of observation, at a regional scale, many rivers can be described as 'distributive fluvial systems' (DFS): a broad, more generalized classification that includes the

sub-classification of 'terminal fluvial fans' (North & Warwick, 2007).

The first detailed model of a distributive fluvial system was introduced by Friend (1978) who recognized three distinctive characteristics: a downstream decrease in river depth, an absence of alluvial incision, and a convex-upward, lobate topography to the river system. Nichols (1987, 1989) and Kelly & Olsen (1993) expanded upon these characteristics and developed conceptual models to describe the sediments, using data from the Miocene of the Ebro Basin, Spain, and Devonian examples from England, Ireland and Greenland. These models have been applied to numerous further examples and refined (e.g. Nichols & Hirst, 1998; Tooth, 2000; Fisher *et al.*, 2007; Nichols & Fisher, 2007), and recent advancements have attempted to quantify their spatial and temporal variations (Hartley *et al.*, 2010; Weissmann *et al.*, 2010, 2013; Owen *et al.*, 2015; Aliyuda & Howell, 2021; Coronel *et al.*, 2020). In general, these studies indicate that distributive fluvial systems are characterized by a radial distributive channel pattern in which channelized flow terminates before a substantial body of water is reached. The preserved deposits of these systems are characterized by a progressive downstream decrease in the dimensions and typically abundance of channel architectural elements, a downstream decrease in the amalgamation of channel-fill elements, and a downstream increase in sheet and floodplain elements, alongside the downstream decrease in grain size displayed by most fluvial systems (Cain & Mountney, 2009, 2011; Hartley *et al.*, 2010; Weissmann *et al.*, 2010, 2013; Owen *et al.*, 2015; Coronel *et al.*, 2020).

This work focusses on distributive fluvial systems that are dominated by dryland rivers in arid to semi-arid climates. These systems are typically characterized by ephemeral to perennial fluvial discharge, and preserved channel elements with high width-to-depth ratios and vertical and lateral connectivity. The preserved deposits of these systems tend to exhibit the following downstream trends: (i) increased dispersal of palaeocurrent directions due to radiating channel patterns from an apex (Owen *et al.*, 2015); (ii) a decrease in modal grain size due to reduced fluvial discharge with an increase in the proportion of floodplain deposits (Weissmann *et al.*, 2010, 2013; Owen *et al.*, 2015); (iii) a decrease in channel element width-to-depth ratios due to channel bifurcation and high rates of infiltration and evapotranspiration into the dry substrate (Horton & DeCelles, 2001; Nichols & Fisher, 2007; Weissmann *et al.*, 2010, 2013; Davidson *et al.*, 2013; Ventra & Clarke, 2018); and (iv) a decrease in the confinement of channel elements due to a lack of lateral constraints on channel mobility (Weissmann *et al.*, 2013; Terwisscha van Scheltinga *et al.*, 2020). Whilst the individual characteristics of this model, when taken in isolation, are true for many types of fluvial system (Sambrook Smith *et al.*, 2010), a combination of all these characteristics forms a strong basis for an interpretation of the system as an ancient dryland DFS (Terwisscha van Scheltinga *et al.*, 2020).

Fluvial systems in dryland settings are commonly ephemeral in nature and are typically characterized by seasonal to strongly intermittent discharge (Mabutt, 1977; Tunbridge, 1984; Billi *et al.*, 2018; Horn *et al.*, 2018) as a result of seasonal and longer-term climatic variations in rainfall (Mather, 2007; Hooke, 2016; Billi *et al.*, 2018). Many sandy ephemeral fluvial systems terminate within muddy flood plains or ephemeral lakes (Tunbridge, 1981; Tunbridge, 1984; Coronel *et al.*, 2020), in a similar fashion to terminal fluvial fans (Nichols, 1987, 1989; Fisher *et al.*, 2007, 2008; Hampton & Horton, 2007; Nichols & Fisher, 2007; Cain & Mountney, 2009; Gulliford *et al.*, 2014; Coronel *et al.*, 2020) and some distributive fluvial systems more generally (Hartley *et al.*, 2010; Weissmann *et al.*, 2010, 2013; Owen *et al.*, 2015).

The fluvial architecture typically comprises sand-bodies representative of sheet-like and channelized elements with high width-to-depth ratios (Williams, 1971; Tunbridge, 1984; Sutfin *et al.*, 2014; Al-Masrahy & Mountney, 2015), which decrease in size downstream and preserve the sedimentary evidence to indicate a progressive downstream decrease in discharge (Babcock & Cushing, 1941; Cornish, 1961; Lane *et al.*, 1971; Mabutt, 1977; Tunbridge, 1984; Sutfin *et al.*, 2014). This is as a result of substantial transmission losses due to high rates of evapotranspiration and infiltration into the surrounding dry substrate (Tooth, 2000; Sutfin *et al.*, 2014). The fluvial architecture varies significantly downstream, with proximal regions characterized by highly amalgamated channels and sheets, and distal regions dominantly characterized by laterally extensive sheet and overbank deposits (Cain & Mountney, 2009, 2011; Hartley *et al.*, 2010; Weissmann *et al.*, 2010, 2013; Owen *et al.*, 2015; Coronel *et al.*, 2020).

The nature of flow within ephemeral systems is highly variable. In addition to cross-strata

produced by Newtonian subcritical flows that are typical of many fluvial systems, non-Newtonian flows tend to generate unconfined sheet-like deposits that display sedimentary textures and structures typical of a high sediment load (Picard & High, 1973; Jaeger *et al.*, 2017), such as structureless sandstones (Horn *et al.*, 2018). Periods of supercritical Newtonian flow, result in antidune cross-strata and upper flow regime plane beds (Long, 2002, 2006; Fielding, 2006), along with some rarer features such as recumbent cross-bedding (Allen & Banks, 1972) and mudballs (Karcz, 1972; Foley, 1978; Bachmann & Wang, 2014). These features are typically described as the product of intermediate to high discharge variance (Fielding *et al.*, 2018).

This study documents the spatial variations in sedimentary architecture of a well exposed, mixed ephemeral fluvial and aeolian system of the Lower Jurassic Kayenta Formation in south-western USA. In so doing, the work explores the processes that likely operated to determine the sedimentology of such a system. It seeks to unravel the complex controls upon the sedimentology to provide insight into the trends in downstream spatial sedimentary architecture that may be attributable to dryland ephemeral fluvial systems, and that could characterize a model for such systems. Consequently, the objectives of this study are: (i) to describe the key characteristic fluvial depositional elements of the system; (ii) to document and quantify spatial distributions and regional variations in fluvial architecture and composition; and (iii) to compare and contrast the results to published distributive fluvial models and unravel potential controls upon deposition.

GEOLOGICAL SETTING

The Kayenta Formation comprises the middle lithostratigraphical unit of the Upper Triassic to Lower Jurassic Glen Canyon Group of the Colorado Plateau in the south-western USA, (Fig. 1) (Pipiringos & O'Sullivan, 1978; Middleton & Blakey, 1983; Dickinson, 2018). The so-called 'J-sub-K' unconformity marks the basal boundary between the Kayenta and underlying Wingate and Moenave formations, whereas the upper boundary of the formation with the overlying Navajo Sandstone is gradational (Riggs & Blakey, 1993; Carpenter & Morales, 1996; Chidsey, 2013; Lucas & Tanner, 2014; Dickinson, 2018).

During the late Triassic to early Jurassic periods, asymmetrical subsidence along the western edge of the Colorado Plateau resulted in two depocentres: the north-east–south-west orientated Utah–Idaho Trough and the north-west–south-east orientated Zuni Sag (Fig. 1) (Bjerrum & Dorsey, 1995; Blakey, 2008; Blakey & Ranney, 2018). Subsidence in both of these depocentres was associated with the development of a retro-arc foreland basin as a result of loading and contraction of the Cordilleran Magmatic Arc and Mogollon Highlands (Fig. 1) towards the south and south-west (Blakey, 2008). The subsequent increase in accommodation space contributed to the preservation of thick successions of strata from the Kayenta Formation and Navajo Sandstone in the west of the Colorado Plateau, that thin dramatically toward the east (Blakey, 1994; Kirkland *et al.*, 2014). Sediments of the Kayenta Formation range in thickness from 28 m in the east of the Plateau, near Cortez, to 460 m in the west, near St. George (Fig. 1).

The Kayenta strata were deposited upon a broad alluvial plain by a dominantly south-westward to westward flowing ephemeral fluvial system sourced from the Uncompahgre Uplift in the Ancestral Rocky Mountains (North & Taylor, 1996), supplemented by a north-westward flowing system sourced from the Mogollon Highlands in the Cordilleran Magmatic Arc (Luttrell, 1993; Hassan *et al.*, 2018). The sediments were deposited dominantly in channel-forms and sheets (Harshbarger *et al.*, 1957; Peterson & Pipiringos, 1979; Bromley, 1991; Luttrell, 1993), and are typically described as a 'sandy' facies in south-eastern Utah and western Colorado and a 'silty' facies in north-western Arizona (Harshbarger *et al.*, 1957). The 'sandy' facies is sourced from the Uncompahgre Uplift (Luttrell, 1993; Hassan *et al.*, 2018) and is characterized by fine to coarse-grained, well sorted sandstones, with minor siltstones and matrix-supported conglomerates (Wilson, 1958). Whereas the 'silty' facies is sourced from both the Cordilleran Magmatic Arc (Luttrell, 1993; Hassan *et al.*, 2018) and the waning fluvial sediment from the Uncompahgre Uplift, and is characterized by reddish purple siltstones, mudstones and minor sandstones (Wilson, 1958).

METHODS

This study is based upon extensive regional sedimentological outcrop logging, and three-dimensional photogrammetric models, to investigate downstream variations in the sedimentary characteristics and interactions between fluvial

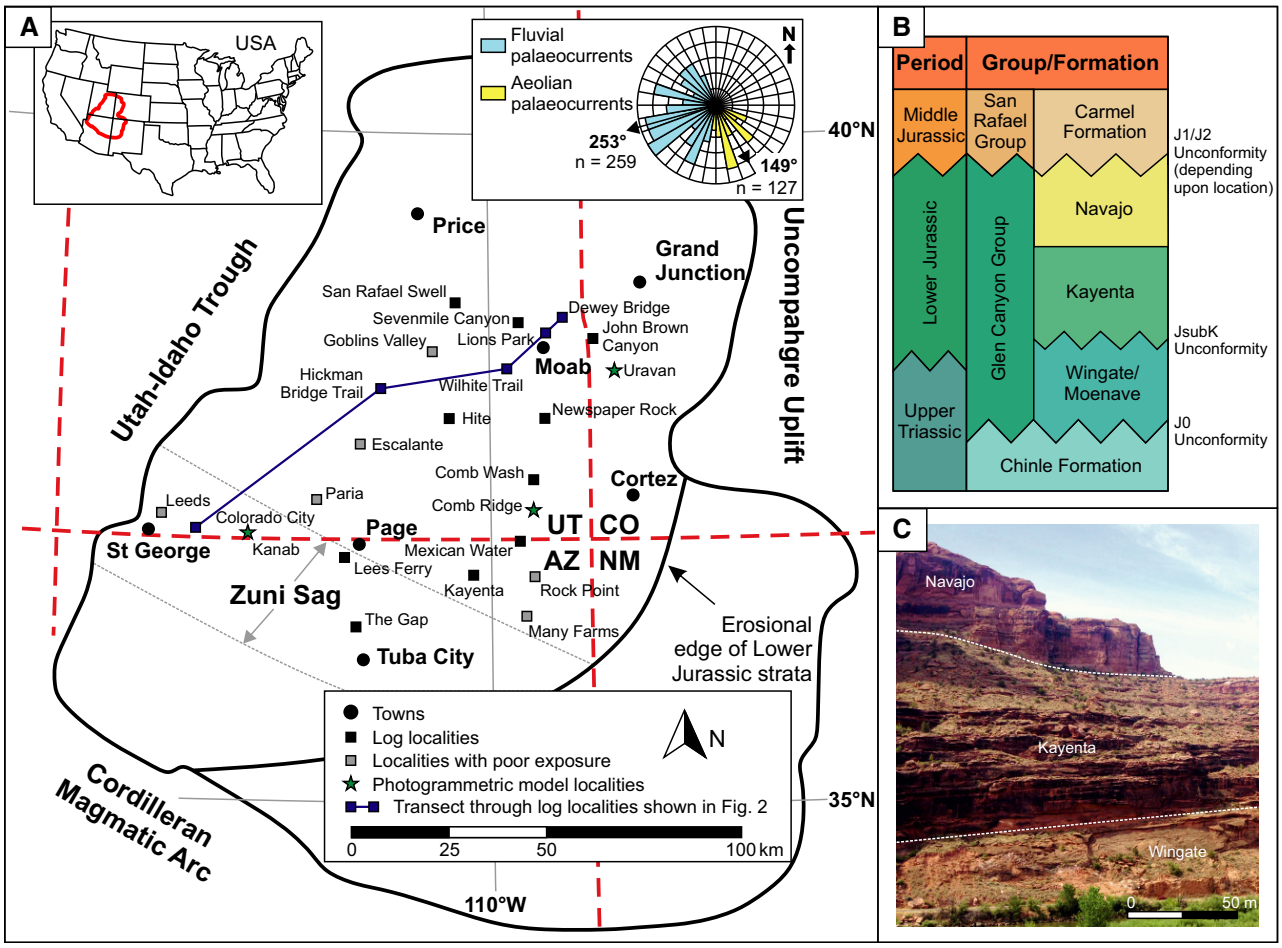

Fig. 1. (A) Location map of the Colorado Plateau and extent of the Kayenta Formation deposition with summary rose diagram illustrating the average palaeoflow directions of both the aeolian and fluvial strata. (B) Stratigraphic column of the Glen Canyon Group. (C) Photograph of the Glen Canyon Group stratigraphy taken along road UT-128 near Lions Park, Moab.

and aeolian deposits during deposition of the Kayenta Formation across the Colorado Plateau.

Twenty-five detailed vertical sections were logged, with a cumulative length of over 1700 m, each spaced laterally approximately 25 km apart, constrained to as close to a grid pattern as exposure allows, over an area of approximately 200 km^2, (Figs 1 and 2). The sedimentary logs record full successions of the Kayenta Formation, from the J-sub-K unconformity to the last main fluvial occurrence within the gradational contact with the overlying Navajo Sandstone. In southern Utah and northern Arizona, this interval includes the basal Springdale Sandstone Member of the Kayenta Formation. The deposits have been classified into proximal, medial and distal sections from the Uncompahgre Uplift, based upon regional changes in fluvial composition and stacking patterns. Proximal deposits are defined by >70% amalgamated channels and <5% overbank, medial deposits are defined by 30 to 70% amalgamated channels and <30% overbank, and distal deposits are defined by <30% amalgamated channels and >30% overbank (Priddy & Clarke, 2020).

Alongside the logs, an extensive palaeocurrent dataset was collected. This dataset comprises 235 measurements from planar and trough cross-bedded foresets, ripple cross-laminated foresets and primary current lineations within fluvial sediments, and 127 measurements from planar and trough cross-bedded foresets within aeolian sediments of the Kayenta Formation.

Three digital photogrammetric models of representative outcrops from proximal, medial and distal fluvial settings (Fig. 3), collected using both a DSLR camera (Nikon D800E; Nikon,

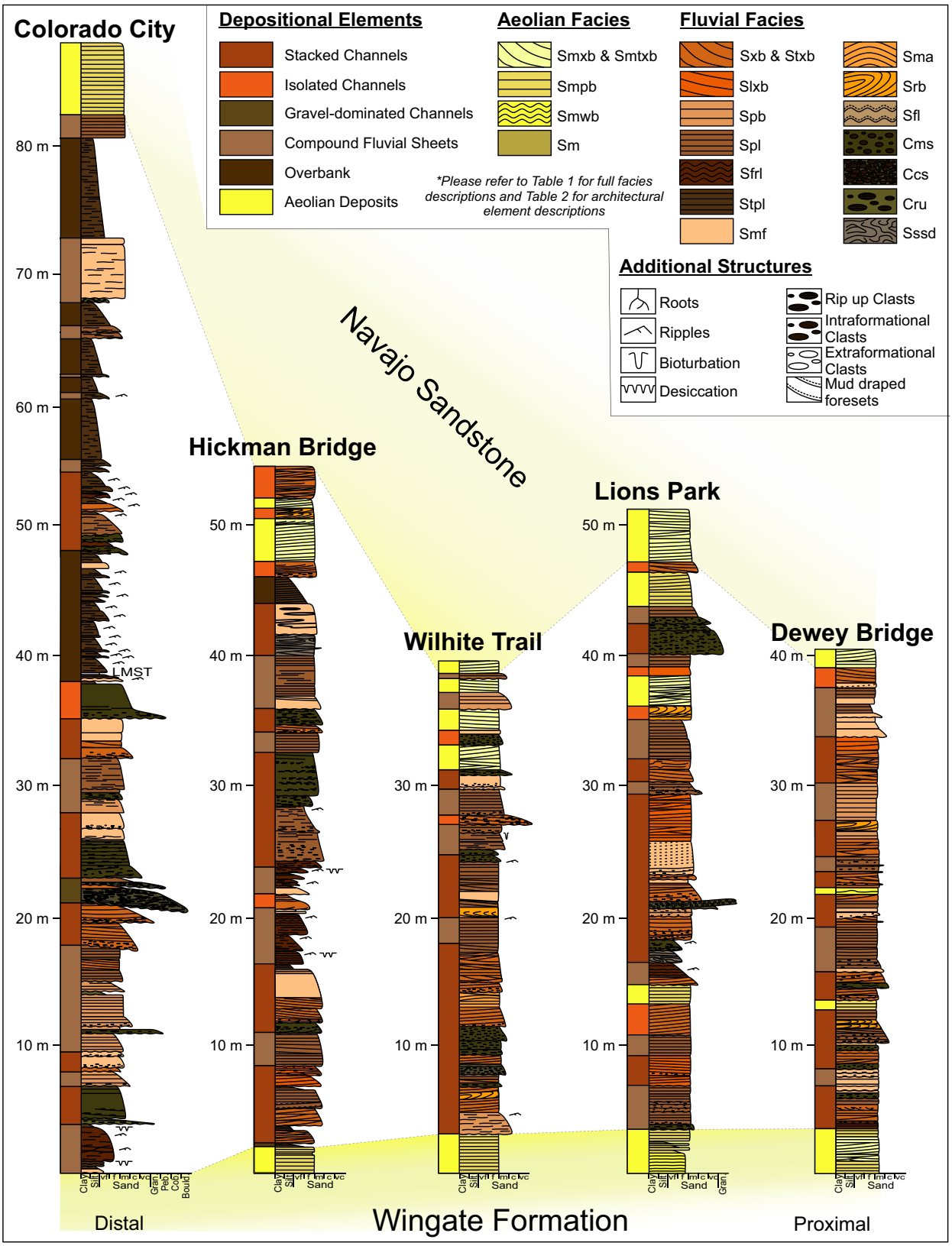

Fig. 2. Representative transect of correlated sedimentary logs through the Kayenta Formation, showing the downstream variations in sedimentology. Sedimentary logs are coloured by lithofacies (see key) with depositional elements colour-coded down the side. See Fig. 1 for line of section and locations.

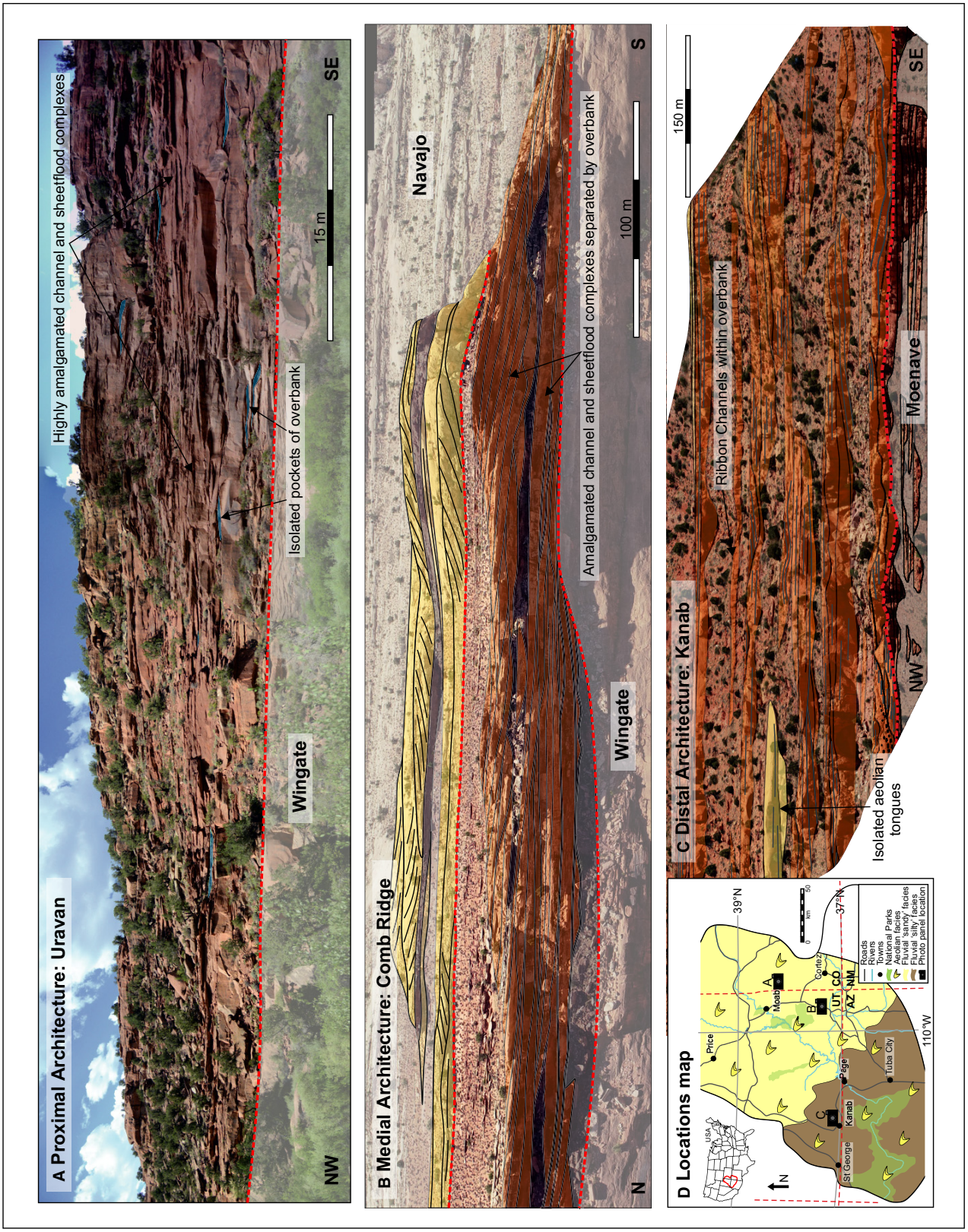
A Proximal Architecture: Uravan
Highly amalgamated channel and sheetflood complexes
Isolated pockets of overbank
Wingate
15 m
NW
SE
B Medial Architecture: Comb Ridge
Navajo
Amalgamated channel and sheetflood complexes separated by overbank
Wingate
100 m
N
S
C Distal Architecture: Kanab
Ribbon Channels within overbank
Isolated aeolian tongues
Moenave
150 m
NW
SE
D Locations map
39°N
37°N
110°W
Price
Moab
Cortez
Page
Tuba City
Kanab
St George
A
B
C
UT
CO
AZ
NM
Roads
Rivers
Towns
National Parks
Aeolian facies
Fluvial sandy facies
Fluvial silty facies
Photo panel location

Fig. 3. Architecture outcrop panels from three locations across the extent of the Kayenta Formation deposition depicting the change in architecture downstream, from highly amalgamated channels and sheets within the proximal to isolated channels and sheets within the distal. (A) Proximal architecture panel of Uravan, Colorado. (B) Medial architecture panel of Comb Ridge, south-east Utah. (C) Distal architecture panel of Kanab, south-west Utah. (D) Locations map illustrating the positions of panels (A) to (C).

Tokyo, Japan) and a drone (DJI Phantom 4 Pro; DJI, Shenzhen, China), were processed in Agisoft PhotoScan®, and analysed using Virtual Reality Geological Studio (VRGS), courtesy of David Hodgetts. Each model comprises between 400 and 600 photographs, with each sedimentary feature pictured in at least five images. Accompanying sedimentary logs along the outcrop face allow for 'ground-truthing' of the sedimentology displayed in the models. The models illustrate: (i) the lateral and vertical relationships between fluvial and aeolian architectural elements; (ii) the geometry and dimensions of the elements; (iii) the nature of contact between the elements; and (iv) differences in architecture and sedimentology between proximal, medial and distal settings.

Using VRGS, the dimensions of the depositional elements were mapped onto the digital outcrop models to determine apparent size of elements in the planes of the models. Palaeocurrent measurements were then used to correct for the orientation of the models and to calculate true element dimensions in directions perpendicular to flow (Visser & Chessa, 2000; Pringle *et al.*, 2010; Rarity *et al.*, 2014). The dimensions of partial or incomplete elements within models have been approximated using methods outlined by Geehan & Underwood (1993). For further detail on the methods of photogrammetric analysis used within this work, the reader is referred to Priddy *et al.*, 2019.

Spatial variations in compositional characteristics; including the thicknesses of fluvial and aeolian strata, along with the percentage of sand, the percentage of conglomerate, and the grain-size distribution of the fluvial sediments, have been calculated and are illustrated as contour maps across the study area. Fluvial and aeolian sediment thicknesses are the total thicknesses of strata of each type observed within the Kayenta Formation at each locality. The percentages of fluvial sand and fluvial conglomerate at each locality were calculated by summing the thicknesses of individual beds of fluvial sediment with average grain sizes of each and comparing these values to the total thicknesses of fluvial sediment at each locality. The average grain size for each locality was calculated from the observed average grain size of each individual bed, with measurements determined per unit thickness in order to normalize by bed thickness.

Analysis of spatial variations in the five identified depositional elements has also been conducted. This includes the percentage of each depositional element per locality, calculated from the total thicknesses of elements of each type displayed in the sedimentary logs, and the average thickness and average grain size of each type of depositional element per locality.

Each contour plot of data is supplemented with a line graph depicting the spatial variations downstream from the Uncompahgre Uplift (following the dominant direction of flow indicated by palaeocurrent data), a line of best fit, and arithmetic averages for the proximal, medial and distal regions. For comparison, secondary lines of best fit are displayed on each contour plot and have been determined by excluding all four distal locations from the analysis. This was done to remove potential effects of sediment derived from the secondary source for the Kayenta – the Mogollon Highlands – from the analysis.

SEDIMENTOLOGY

Twenty-one facies have been identified within the Kayenta Formation. Five facies are interpreted as the product of wind-blown processes; the remaining 16 facies are interpreted as the product of sub-aqueous processes. The facies are typical of those found in aeolian and ephemeral braided fluvial deposits, and their descriptions concur with those of previous workers (Hunter, 1977; Miall, 1988; Langford & Chan, 1989; Kocurek, 1991; North & Taylor, 1996; Hassan *et al.*, 2018). Consequently, for the sake of brevity, the facies are summarized in Table 1.

The 21 facies form nine architectural elements, for which detailed descriptions are given in Priddy & Clarke (2020) and key characteristics are summarized in Table 2. Combinations of the

Table 1. Summary of lithofacies observed in the Kayenta Formation modified from Priddy & Clarke (2020).

Code	Lithology and texture	Sedimentary structures	Interpretation
Smxb	Grey to orange, fine to medium-grained, well sorted and well rounded sandstone	Planar cross-bedding with millimetre/centimetre scale alternations in grain size in single or multiple sets, sporadic soft sediment deformation	Migration of wind-blown straight-crested dune-scale bedforms and dune trains. Soft sediment deformation formed as a result of loading on a damp substrate
Smtxb	Grey to orange, fine to medium-grained, well sorted and well rounded sandstone	Trough cross-bedding with millimetre/centimetre scale alternations in grain size in single or multiple sets, sporadic soft sediment deformation	Migration of wind-blown sinuous-crested dune-scale bedforms and dune trains. Soft sediment deformation formed as a result of loading on a damp substrate
Smpb	Grey to orange, fine to medium-grained, well sorted and well rounded sandstone	Planar-bedding with millimetre scale alternations in grain size	Wind-blown deposits formed by the deflation of dune-scale bedforms
Smwb	Grey to orange, fine to medium-grained, well sorted and well rounded sandstone	Undulose-laminations with millimetre scale alternations in grain size	Migration of wind-blown ripple-scale bedforms, producing pinstripe laminae
Sm	Grey to orange, very fine to medium-grained, well sorted and well rounded sandstone	Structureless, sporadic desiccation cracks and bioturbation	Suspension settling of wind-blown sediment in areas affected by surface water, followed by drying
Sxb	Brown medium-grained, moderate/well sorted and sub-rounded/well rounded sandstone	Planar cross-bedding with normal grading, in single or multiple sets, sporadic clasts, mud draping and soft sediment deformation	Migration of straight-crested dune-scale bedforms and dune trains sub-aqueously under lower flow regime conditions with high sediment load
Stxb	Brown medium-grained, moderate/well sorted and sub-rounded/well rounded sandstone	Trough cross-bedding with normal grading, in single or multiple sets, sporadic clasts and soft sediment deformation	Migration of sinuous-crested dune-scale bedforms and dune trains sub-aqueously under lower flow regime conditions
Slxb	Brown medium-grained, moderate/well sorted and sub-rounded/well rounded sandstone	Low-angle cross-bedding in single or multiple lenticular sets and sporadic reactivation surfaces	Lateral migration of macro-forms in lower flow regime conditions
Spb	Brown medium-grained, moderate/well sorted and sub-rounded/well rounded sandstone	Planar-bedding, sporadic clasts	Sub-aqueous upper flow regime flat beds
Spl	Brown fine to medium-grained, moderate/well sorted and sub-rounded/well rounded sandstone	Parallel laminations	Sub-aqueous upper flow regime flat beds
Sfrl	Brown siltstone to medium-grained, moderate/well sorted and sub-rounded/well rounded sandstone	Ripple cross-laminations, with sub-critically to super-critically climbing multiple sets which form cosets	Migration of ripple-scale bedforms in lower flow regime
Smf	Orange to brown medium-grained, moderate/well sorted and sub-rounded/well rounded sandstone	Structureless, sporadic clasts concentrated in basal sections	Rapid deposition in high sediment load suppressing bedform development
Sma	Orange to brown medium-grained, moderate/well sorted and sub-rounded/well rounded sandstone	Sigmoidal-bedding with normally graded foresets in single or multiple sets	Upper flow regime – antidune development

Table 1. (continued)

Code	Lithology and texture	Sedimentary structures	Interpretation
Srb	Orange to grey medium-grained, moderate/well sorted and sub-rounded/well rounded sandstone	Recumbent cross-bedding, sporadic mud draping on foresets in single or multiple sets, with slightly concave set bounding surfaces	Migration of sinuous-crested dune-scale bedforms in lower flow regime with high sediment load
Sfl	Brown siltstone to fine-grained sub-arkosic arenite	Flaser laminations with silt lining foreset and set bounding surfaces	Migration of ripple-scale bedforms in lower flow regime/ waning flow conditions
Sssd	Purple to brown siltstone to fine-grained sandstone matrix, with locally derived sediment, forming moderate/poorly sorted and sub-rounded clasts	Soft sediment deformed clasts with silt lining the contorted foresets and between the deformed clasts	Sub-aqueous mass transport deposits: debris flow/slumping/ sliding into a high sediment load flow
Stpl	Dark brown siltstone, sporadic mottling	Parallel to faint undulose laminations, sporadic rhizoliths, desiccation cracks and bioturbation	Suspension fall out from stationary waters. Stabilization for vegetation to develop
Cms	Grey to brown medium-grained sand to pebble-grade, polymictic conglomerate, poorly sorted, sub-rounded, matrix-supported	Structureless to sporadic crude trough cross-bedding, with abundant clasts lining foresets	Sub-aqueous lower flow regime conditions with high sediment load, intermittent development and migration of dune-forms
Ccs	Grey to brown coarse-grained sand to pebble-grade, polymictic conglomerate, poorly sorted, sub-rounded, clast-supported	Structureless to very crude cross-bedding, abundant clasts throughout	Sub-aqueous, high energy Newtonian flow under high sediment load conditions, with suppressed bedform development
Cru	Grey to orange medium-grained, poorly sorted, sub-rounded/sub-angular, matrix-supported. Rip-up clasts ranging from granule to cobble grade	Structureless to very sporadically crudely cross-bedded, rip-up clasts at base	Sub-aqueous high energy flow under high sediment load conditions and reworking of locally derived sediment
Lm	Grey siliciclastic rich, carbonate wackestone with sporadic red chert	Structureless to undulose laminated	Sub-aqueous precipitation of allochthonous carbonate with siliciclastic input

Abbreviations: Ccs, Sub-aqueous clast-supported conglomerate; Cms, Sub-aqueous matrix-supported conglomerate; Cru, Sub-aqueous rip-up clast conglomerate; Lm, Sub-aqueous siliciclastic-rich limestone; Sfl, Sub-aqueous flaser laminated sandstone; Sfrl, Sub-aqueous ripple cross-laminated sandstone; Slxb, Sub-aqueous low-angle cross-bedded sandstone; Sm, Sub-aerial structureless sandstone; Sma, Sub-aqueous sigmoidal bedded sandstone; Smf, Sub-aqueous structureless sandstone; Smpb, Sub-aerial planar-bedded sandstone; Smtxb, Sub-aerial trough cross-bedded sandstone; Smwb, Sub-aerial undulose laminated sandstone; Smxb, Sub-aerial planar cross-bedded sandstone; Spb, Sub-aqueous planar-bedded sandstone; Spl, Sub-aqueous parallel laminated sandstone; Srb, Sub-aqueous recumbent cross-bedded sandstone; Sssd, Sub-aqueous soft sediment deformed sandstone; Stpl, Sub-aqueous parallel-laminated siltstone; Stxb, Sub-aqueous trough cross-bedded sandstone; Sxb, Sub-aqueous planar cross-bedded sandstone.

nine architectural elements occur in differing arrangements and they can be classified into five key larger-scale fluvial depositional elements, each one representing a major component of the overall system. Each deposition element is described below (Figs 4 and 5).

Amalgamated sandstone-dominated channel-fill

Laterally and vertically amalgamated sandstone-dominated channel-fill depositional elements comprise predominantly channel and accretionary

Table 2. Summary of architectural elements modified from Priddy & Clarke (2020).

Element	Code	Facies	Description
Aeolian dune	AD	Smxb, Smtxb, Smpl, Smwb	Tabular bodies with lateral extents up to 300 m and vertical extents up to 150 m
Sandsheet	SS	Smpl, Smwb, Sm	Tabular bodies with lateral extents over hundreds of metres and vertical extents up to 3 m
Interdune	AI	Sm, Spl, Sfrl, Stpl	Lensoidal or sheet-like bodies with lateral extents up to 20 m and vertical extents up to 2 m
Fluvial channel	FC	Cms, Ccs, Cru, Sxb, Stxb, Spl, Srb, Smf	'U' shaped elements with lateral extents up to 115 m and vertical extents up to 4 m
Sheetflood	SF	Cru, Spb, Sma, Smf, Spl, Sfrl, Sfl	Tabular bodies with lateral extents between 250 m and 400 m and vertical extents up to 5 m
Lateral accretion	LA	Stxb, Slxb, Spl, Sfrl	Lensoidal elements with lateral extents up to 100 m and vertical extents up to 3 m
Downstream accretion	DA	Cms, Sxb, Slxb, Srb, Spl, Sfrl	Lensoidal elements with lateral extents up to 200 m and vertical extents up to 4 m
Bank collapse	BC	Sssd, Stpl	Tabular bodies with lateral extents up to 20 m and vertical extents up to 3 m
Overbank	OB	Stpl, Spl, Lm	Tabular bodies, rarely preserved with lateral extents up to 10 m and vertical extents up to 4 m

architectural elements (Fig. 5; Table 2) and occur primarily within the proximal and medial regions of the Kayenta Formation, with the degree of element amalgamation decreasing downstream towards the south-west. Small, isolated lenses of overbank are sporadically observed between stacked channel architectural elements. Examples of the depositional element typically form large laterally extensive sheet-like complexes, which are up to 0.5 km wide in directions perpendicular to palaeoflow, and up to 25 m thick.

Channelized architectural elements present within this larger depositional element are dominated by successions of medium-grained planar to trough cross-bedded sandstones (Sxb and Stxb) with conglomeratic basal lags and sporadic very coarse to granule-grade clasts lining crudely developed foresets. The uppermost strata of the channel elements comprise structureless (Smf) to parallel-laminated (Spl) sandstones. The accretionary elements within this depositional element are dominated by successions of medium-grained low-angle cross-bedded sandstones (Slxb) and sporadic planar (Sxb), trough (Stxb) and recumbent (Srb) cross-bedded sandstones, with the tops of the successions comprising ripple cross-laminated sandstones (Sfrl).

Amalgamated sandstone-dominated channel-fill depositional elements represent extensive erosive channel complexes (Gibling, 2006) that extended over the proximal and medial regions during periods of increased fluvial activity (*cf.* Cain & Mountney, 2009). The development of the sheet-like bodies of amalgamated channels most probably resulted from the repeated avulsion of channels across a common stratigraphical horizon, cannibalizing any overbank that developed (Mackey & Bridge, 1995; Miall, 1996; Bridge, 2003; *cf.* Cain & Mountney, 2009). The individual channel-fills are dominated by facies indicative of accumulation via bedload transport and deposition under conditions of high flow velocity and sediment load (Bridge, 2006). The vertical arrangement of facies, with no clear fining-upward trend, suggests deposition in a flow with a strongly fluctuating sediment load, from which only minimal evidence of waning flow is preserved in the sedimentology (Priddy & Clarke, 2020). This interpretation is supported by pebble and mud-lined foresets which, along with the abundance of upper flow regime plane beds, suggest deposition within a river with episodic discharge (Miall, 1977; Stear, 1985; Lorenz & Nadon, 2002; Owen *et al.*, 2015).

Depositional Element	Description	Elements contained	Dimensions	Occurrence	
Amalgamated sandstone-dominated channel-fill	Large laterally extensive sheet-like complexes with erosional 5th order basal bounding surfaces	FC, LA, DA	Up to 25 m thick, with lateral extents up to 500 m	Predominantly within proximal and medial regions with decreased stacking towards the distal	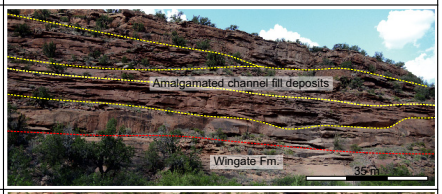
Isolated sandstone-dominated channel-fill	Lensoidal bodies with erosional 5th order basal bounding surfaces	FC	Between 0.5 m and 4 m thick, with lateral extents up to 115 m	Proximal, medial and distal regions	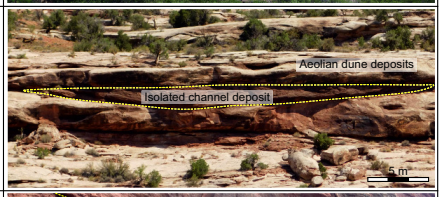
Isolated gravel-dominated channel-fill	Laterally extensive highly erosional elements with steep sides and basal 5th order bounding surfaces	FC	1 - 2 m thick, with lateral extents up to 50 m	Proximal, medial and distal regions	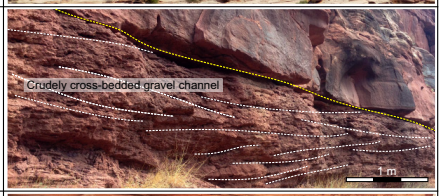
Compound sandstone-dominated fluvial sheets	Lensoidal to sheet-like bodies with erosional 5th order basal bounding surfaces	SF	Up to 20 m thick, with lateral extents up to 750 m	Proximal, medial and distal regions, with decreased stacking towards the distal	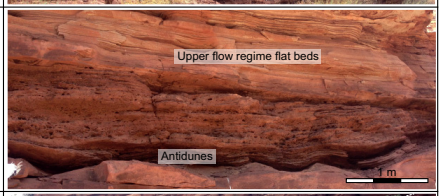
Overbank	Isolated lenses to laterally extensive tabular bodies	OB, SF	5 - 20 cm thick lenses with widths of 2 m, 2 - 15 m thick bodies with lateral extents over 100s metres	Predominantly within distal regions	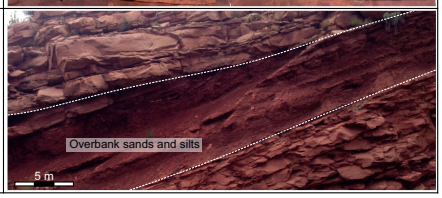

Fig. 4. Summary table of fluvial depositional elements within the Kayenta Formation.

Isolated sandstone-dominated channel-fill

Isolated sandstone-dominated channel-fill depositional elements comprise predominantly channel architectural elements (Fig. 5; Table 2) and occur within proximal, medial and distal areas of the Kayenta Formation. In proximal and medial areas, the isolated depositional elements of this type are preserved sporadically between compound sandstone-dominated fluvial sheet deposits, but in the distal setting they are dominantly preserved within overbank deposits. The depositional elements have a lensoidal channel geometry, 0.5 to 4.0 m thick in sections perpendicular to flow, with lateral extents up to 115 m, and a dominant palaeocurrent towards the south-west. Within the proximal and medial regions, the isolated channel-fill depositional elements are dominated by medium-grained low-angle cross-bedded (Slxb) and planar-bedded (Spb) to parallel-laminated (Spl) sandstones with a conglomeratic basal lag. Distal equivalents of these isolated channel elements are dominated by generally finer grained, structureless (Smf) to parallel-laminated (Spl) sandstones with rip-up-clast-dominated conglomeratic bases.

Isolated sandstone-dominated channel-fill depositional elements represent the deposits of largely fixed fluvial channels, typically termed ribbon channels (e.g. North & Taylor, 1996), which are generally stable and exhibit little lateral migration (*cf.* Friend *et al.*, 1979; Gibling, 2006; Cain & Mountney, 2009; Owen *et al.*, 2015). They occur along the same stratigraphical horizon, which may be due to the divergence of the active channel in a distributary network (Kelly & Olsen, 1993; Nichols & Fisher, 2007),

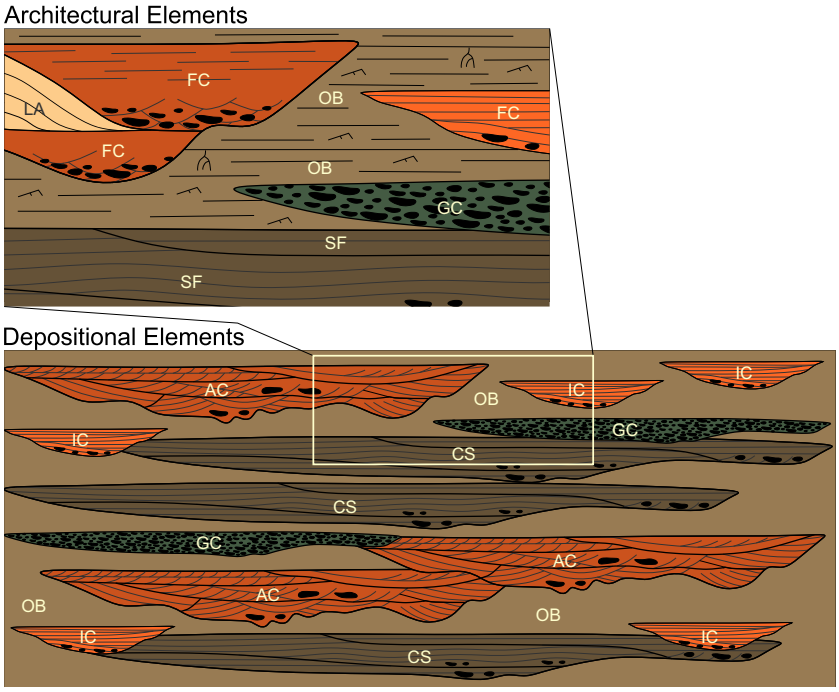

Fig. 5. Representation of the internal composition, architecture, and geometries of the large-scale depositional elements. Architectural elements: FC, fluvial channel; LA, lateral accretion; GC, gravel-dominated channel; SF, fluvial sheet; OB, overbank. Depositional elements: AC, amalgamated sandstone-dominated channel-fill; IC, isolated sandstone-dominated channel-fill; GC, isolated gravel-dominated channel-fill; CS, compound sandstone-dominated fluvial sheet; OB, overbank.

the re-convergence and divergence of an anabranching channel pattern (Nanson & Knighton, 1996; Tooth & Nanson, 1999; Bridge, 2003), or a situation in which each isolated channel represents abandonment following avulsion and therefore each isolated channel element represents the deposits of channels that would not have been coevally active (Bridge, 2006; North & Warwick, 2007). Planform channel patterns are difficult to determine within the Kayenta Formation. Consequently, any of these processes may be responsible for depositing isolated channel depositional elements, but the ephemeral nature of the system suggests that the latter process is more probable.

Isolated gravel-dominated channel-fill

Isolated gravel-dominated channel-fill depositional elements occur across the extent of Kayenta deposition, with the most prominent examples observed within the medial and distal regions. Each example of this depositional element is typically 1 to 2 m thick with lateral extents, in a direction perpendicular to flow, of tens of metres, or more. They are characterized by erosive basal bounding surfaces and lateral pinch-out displaying steep, near vertical profiles, and a representative succession dominantly composed of structureless to crudely cross-bedded clast-supported intraformational conglomerates (Ccs), fining-upward into structureless (Smf) to parallel-laminated (Spl) sandstones. The intraformational sediment in proximal and medial settings is dominantly composed of sub-lithic arenite and argillaceous material, with a minor calcareous content. The argillaceous and calcareous components increase towards the distal region.

Isolated gravel-dominated channel-fill depositional elements were deposited by high-energy fluvial channel discharge events that occasionally traversed into the distal alluvial plain (*cf.* Cain & Mountney, 2009). Within the proximal to medial regions, the presence of intraformational arenaceous clasts within individual channel elements suggests that the fluvial system eroded into adjacent non-cohesive sandy overbank/floodplain areas (Gómez-Gras & Alonso-Zarza, 2003). Within the distal region, abundant argillaceous and calcareous clasts suggest erosion of a silt-dominated floodplain with an indurated calcrete crust. The crude cross-bedding within the conglomeratic fill indicates periods of high flow velocities that were prolonged enough for some in-channel bedform development and migration (Williams, 1970), but generally the large sediment grain size prevented bedload transport and the development of migrating bedforms. The structureless nature of overlying sandstones suggests rapid deposition from a system with a high sediment load that prevented the formation of bedforms (Bridge & Best, 1988; Todd, 1996).

Compound sandstone-dominated fluvial sheets

Compound sandstone-dominated fluvial sheet depositional elements occur across the expanse of the Kayenta, with high degrees of amalgamation in the proximal to medial regions, decreasing towards the distal setting. Examples of this depositional element are up to 1 km wide in directions perpendicular to a south-west palaeoflow, and up to 20 m thick.

Sheet-like architectural elements (Fig. 5; Table 2) within this larger depositional element are dominated by medium-grained structureless sandstones (Smf) and planar-bedded (Spb) to sigmoidal-bedded (Sma) sandstones with basal rip-up clast conglomerates (Cru), with sporadic very coarse to granule (up to 30 cm along the long axis) sized rip-up clasts lining crudely developed foresets. The top of the element comprises parallel-laminated (Spl) to ripple cross-laminated (Sfrl) sandstones.

Compound sandstone-dominated fluvial sheet depositional elements are attributed to the unconfined flow of flood waters across the alluvial plain (*cf*. Cain & Mountney, 2009). The un-channelized nature of the internal sheet-like elements probably initiated from breaches of the banks of active channels during times of high flow velocities (Tooth, 2000, 2005). Each individual fining-upward element with an erosive base represents an individual flood event (Miall, 1996, 2014) within which the arrangement of facies in a vertical succession dominated by the preservation of upper flow regime structures suggests deposition within a high velocity flow that waned quickly (Williams, 1971). Ripple-laminated sandstones suggest that flow waned enough for ripple-scale bedform development and migration; however, sediment supply was still significant enough to promote supercritical climb.

Overbank

Overbank depositional elements are most prominent within the distal region and comprise overbank and sheet-like architectural elements (Fig. 5; Table 2) of Priddy & Clarke (2020). The depositional element is dominated by parallel-laminated to faintly rippled siltstones (Stpl), parallel-laminated sandstones (Spl) and structureless to undulose laminated siliciclastic-rich carbonate wackestones (Lm), with the proportion of each facies varying throughout the succession and depositional area. In the proximal region, preserved overbank depositional elements are very sporadic and do not exceed thicknesses of 1 m, but rip-up clasts of overbank material within fluvial channel and sheet architectural elements attest to probable greater overbank development than that preserved may suggest. Similar observations hold true for the medial setting, but with a slight increase in abundance of the depositional element. Here, the depositional element attains thicknesses of up to 5 m and is dominated by parallel-laminated sandstone (Spl) and parallel-laminated to faintly rippled siltstone (Stpl). Overbank depositional elements comprise a significant proportion of the distal region with mottling, bioturbation, rhizoliths and desiccation cracks being typical features within the parallel-laminated to faintly rippled siltstone (Stpl). Occurrences of the depositional element generally range in thickness from 2 to 10 m, but sporadically reach in excess of 15 m. Isolated lenses of structureless to undulose laminated siliciclastic rich carbonate wackestone (Lm) are abundant within this depositional element in the distal setting, forming as thin and laterally extensive sheets, generally 5 to 20 cm thick and 2 m wide.

Overbank depositional elements resulted from unconfined flow when the discharge exceeded the bank-full capacity of the channel network (Bridge, 2003; *cf*. Cain & Mountney, 2009). Preservation of this depositional element is generally poor due to reworking and erosion by other depositional elements, except for thick deposits near top of formation, which contain desiccation cracks and rhizoliths indicating stabilization and drying of the floodplain (Miall, 1988), and within the distal region, indicating waning of flow and channel abandonment. Isolated siliciclastic-rich carbonate wackestone lenses result from entrapment of water in small depressions for relatively long periods of time after the fluvial system wanes (Allen, 1974; Pettigrew *et al*., 2019).

GENERAL SPATIAL VARIATIONS OF THE KAYENTA FORMATION

Spatial variations in the architecture, cumulative thickness, composition and grain size of the Kayenta have been analysed across the expanse of the study area. The results focus on the data derived from the dominant south-westward flowing fluvial system sourced from the Uncompahgre Uplift. However, data from the second north-westward flowing axial system have been

highlighted and the effects on the downstream trends are addressed within the discussion.

Architecture of the Kayenta Formation

The proximal region of the fluvial Kayenta system around Moab, Utah, comprises a series of laterally and vertically amalgamated sandstone-dominated channel-fill depositional elements with abundant compound sandstone-dominated fluvial sheet depositional elements, but very few overbank depositional elements (Fig. 3A).

Lateral and vertical amalgamation of channel depositional elements decreases by the medial region of the system (around Comb Ridge, Utah), but compound sandstone-dominated fluvial sheet depositional elements are still abundant and extend laterally for over 400 m (Fig. 3B). Channel depositional elements are typically isolated within compound sandstone-dominated fluvial sheet depositional elements, and overbank depositional elements are prevalent between channels and compound fluvial sheets.

The distal region around Kanab, Utah, consists of isolated sandstone-dominated channel and compound sandstone-dominated fluvial sheet depositional elements preserved within overbank depositional elements (Fig. 3C). Compound sandstone-dominated fluvial sheet depositional elements form at distinct stratigraphic levels within the overbank to provide a relatively low degree of sandstone connectivity.

Thickness variations within the Kayenta Formation

The total thickness of the fluvial strata shows a gradual increase downstream, but with an abrupt thickening over a short distance within the distal region (62 m of fluvial sediment at Lees Ferry, compared to 154 m at Kanab, just 85 km away) (Fig. 6A and B). The thickness of the fluvial component of the succession also generally decreases towards the north-west and the south-east, perpendicular to palaeoflow. However, omitting the data within the distal region that may be influenced by the secondary source, reveals an opposing trend, with cumulative fluvial sediment thickness decreasing downstream (Fig. 6A and B).

The coeval aeolian deposits also show a gradual increase in thickness with respect to downstream distance of the fluvial system, again with an abrupt thickening over a short distance within the distal region (Fig. 6C and D). However, in relation to the prevailing east to south-east palaeowind direction (determined from the palaeocurrent measurements of the coeval aeolian deposits) the thickness of aeolian sediment generally decreases down-wind, particularly within the medial region.

Composition of the Kayenta Formation

The percentage of sand within the fluvial system decreases downstream towards the south-west (Fig. 6E and F) from up to 100% in the proximal region (Dewey Bridge, UT, and John Brown Canyon, CO) to 58% distally (The Gap, UT). Slightly anomalous sandstone percentages are observed within some medial sections (Kayenta, AZ – 95%; Mexican Water, UT – 96%), as well as Lees Ferry in the distal region (88%), but these values fit the general trend of a decrease in sandstone percentage towards the south-west. In the medial region, a progressive downstream reduction in the fraction of sandstone within the system is accompanied by a downstream increase in the proportion of siltstone from approximately 1 to 17%. However, within the distal region the progressive downstream reduction in the fraction of sandstone is accompanied by a progressive increase in both siltstone (9 to 34%) and conglomerates (3 to 8%) (Fig. 6G and H).

Overall grain size of the Kayenta Formation

The average grain size of all fluvial sediment, irrespective of the depositional element in which it is preserved, gradually decreases downstream from dominantly medium-grained sandstone within the proximal region to fine-grained to very fine-grained sandstone within the distal region (Fig. 6I and J). The average grain size also decreases radially from the dominant trend. A few anomalies are present, in particular, at Lees Ferry within the distal region where the largest average grain size (1.26ϕ) of the whole system is observed. Despite local anomalies, a clear downstream fining is present.

ANALYSIS OF THE DEPOSITIONAL ELEMENTS

Spatial variations in distribution, thickness and grain size for each depositional element have been analysed across the expanse of the study area. The results focus on the data derived from the dominant south-westward flowing fluvial system sourced from the Uncompahgre Uplift. However, data from the second north-westward

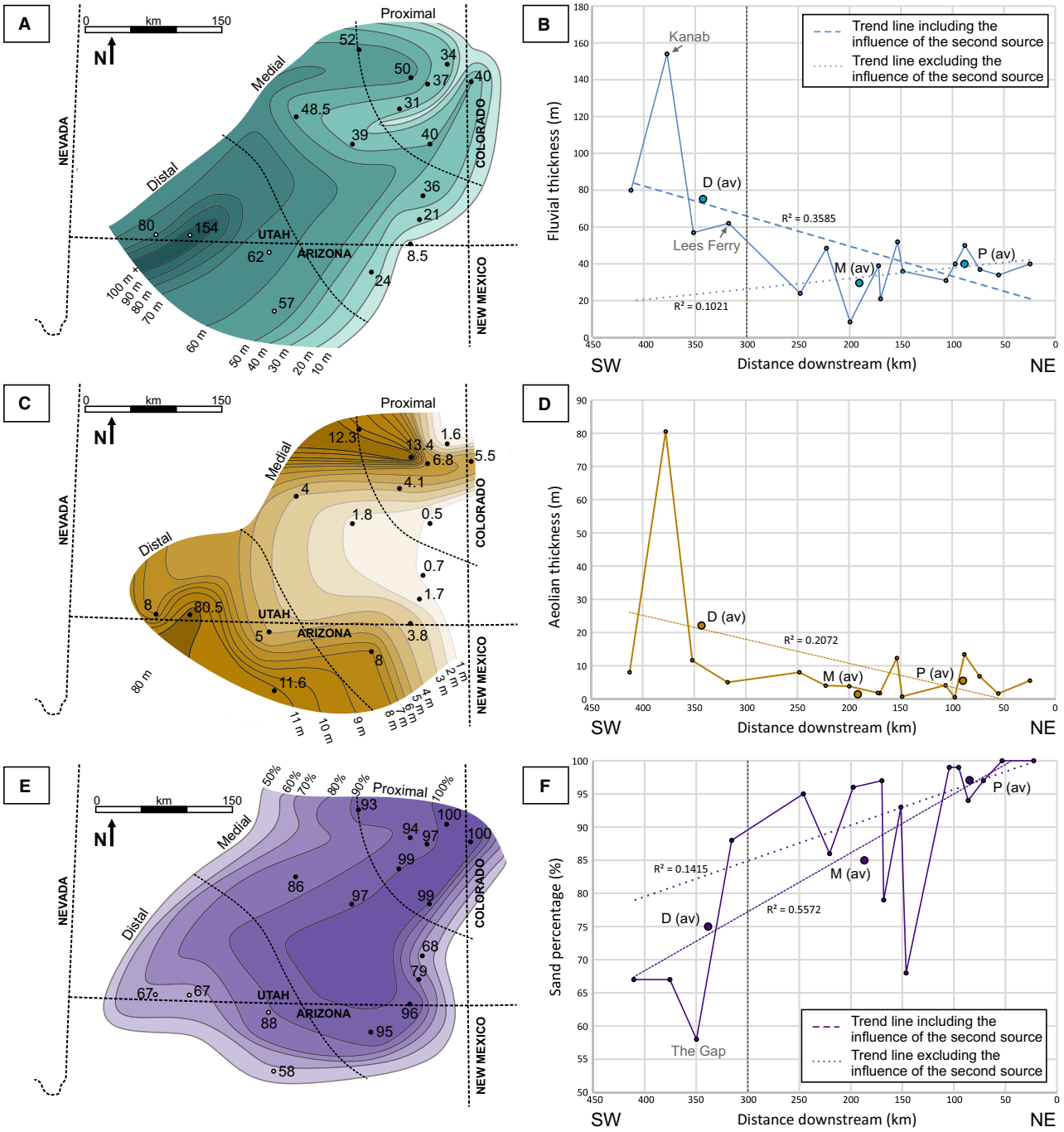

Fig. 6. (A) Contour map of fluvial sediment thickness at each locality. (B) Graph of total fluvial sediment thickness against distance downstream. (C) Contour map of aeolian sediment thickness at each locality. (D) Graph of total aeolian sediment thickness against distance downstream. (E) Contour map of sand percentage at each locality. (F) Graph of sand percentage against distance downstream. (G) Contour map of conglomerate percentage at each locality. (H) Graph of conglomerate percentage against distance downstream. (I) Contour map of the average grain size (Φ) at each locality. (J) Graph of average grain size (Φ) against distance downstream. Average measurements of proximal, medial and distal portions are denoted as P (av), M (av) and D (av) on each graph. Dashed line in each case is a linear best fit to the total dataset and the dotted line is a linear best fit line excluding the data influenced by the secondary fluvial source.

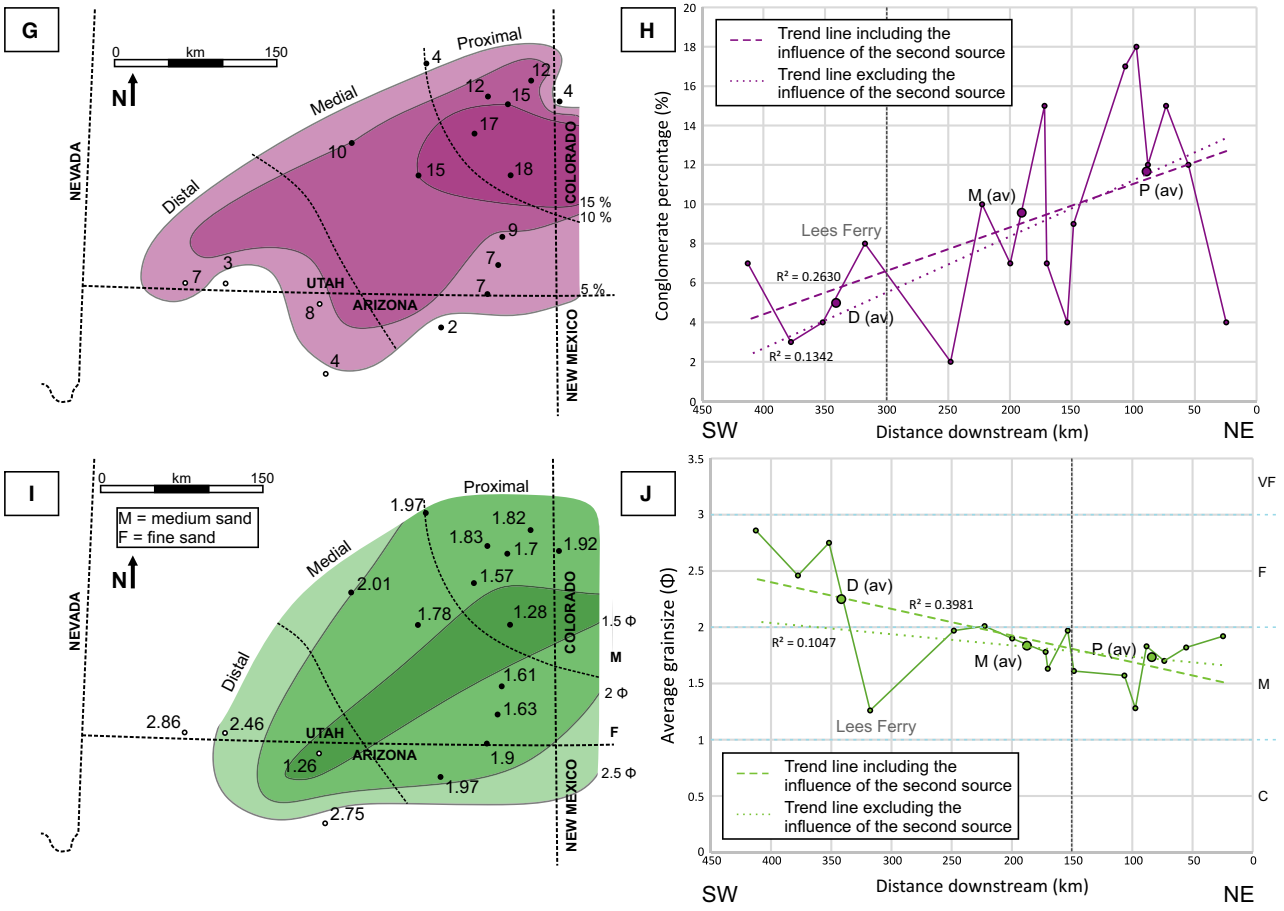

Fig. 6. Continued

flowing axial system have been highlighted and the effects on the downstream trends are considered within the discussion.

Distribution of depositional elements

The relative proportions of both amalgamated sandstone-dominated channel-fill (Fig. 7A and B) and overbank (Fig. 7I and J) depositional elements display strong downstream trends and radial patterns. Weaker trends are present for isolated sandstone-dominated channel-fill (Fig. 7C and D), isolated gravel-dominated channel-fill (Fig. 7E and F) and compound sandstone-dominated fluvial sheet depositional elements (Fig. 7G and H).

The proportions of overbank depositional elements increase with distance downstream (Fig. 7I and J), with the lowest proportions preserved within the central proximal region (John Brown Canyon, Dewey Bridge, Lions Park, Wilhite Trail and Hite). Downstream, in the medial region, overbank depositional elements become more prevalent to constitute between 1% of the fluvial sediments at Newspaper Rock and up 35% of the succession at Comb Ridge. Between 36% (Colorado City) and 44% (The Gap) of the fluvial sediments in the distal region are overbank depositional elements.

By contrast, the proportions of amalgamated sandstone-dominated channel-fill depositional elements decrease with distance downstream (Fig. 7A and B). The highest proportions are preserved in the fluvial sediments of the central proximal region, particularly those of Newspaper Rock (76%) and San Rafael Swell (71%). Downstream, the amalgamated sandstone-dominated channel-fill depositional elements decrease in abundance to constitute between 30% (Comb Ridge) and 69% (Hite) of the fluvial sediments by the medial region, and between

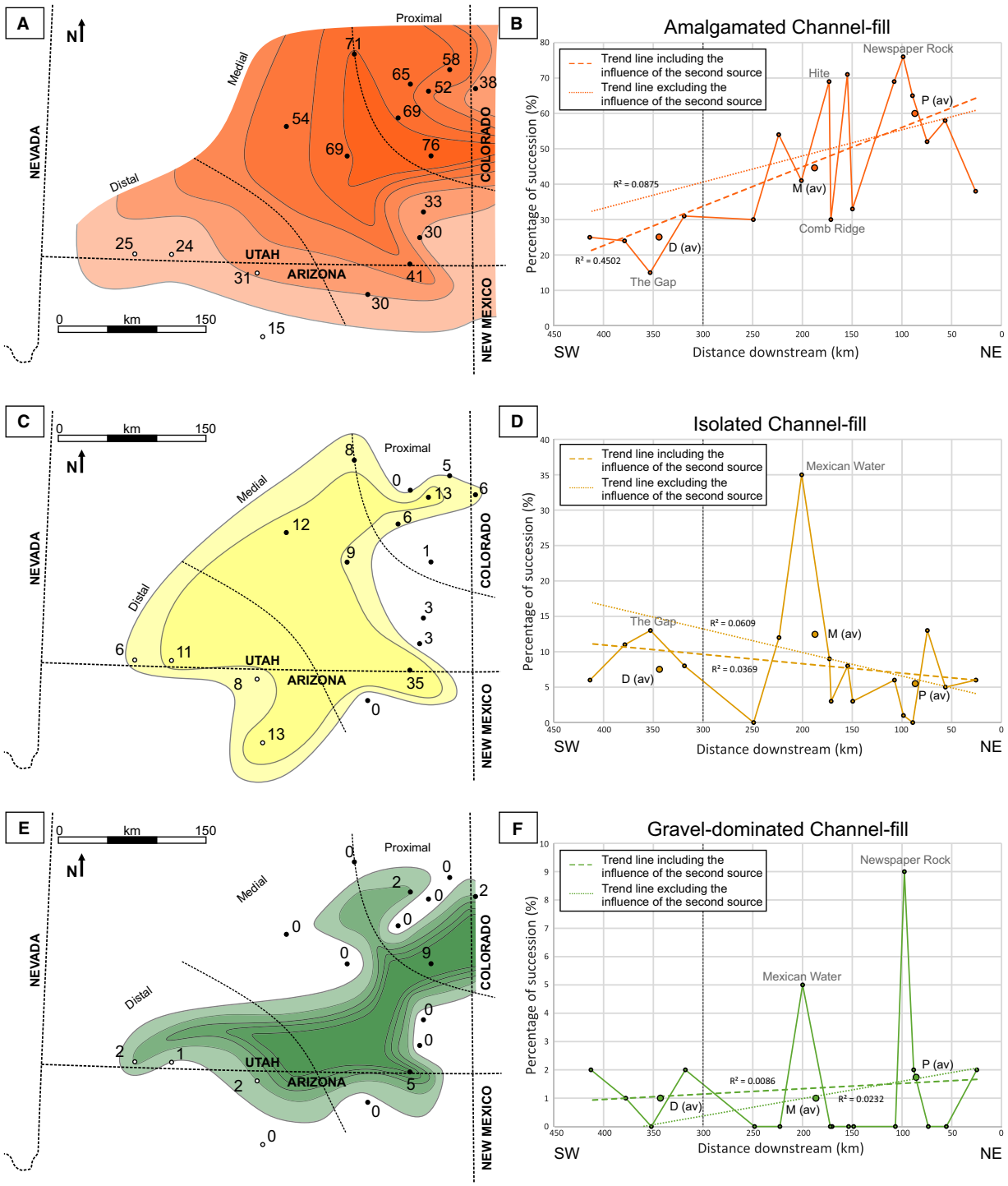

Fig. 7. Contour maps and graphs illustrating the percentage that each depositional element constitutes of the whole fluvial succession at each locality. (A) Amalgamated channels contour map. (B) Graph of amalgamated channel percentage against distance downstream. (C) Isolated channels contour map. (D) Graph of isolated channel percentage against distance downstream. (E) Gravel-dominated channel contour map. (F) Graph of gravel-dominated channel percentage against distance downstream. (G) Compound fluvial sheet contour map. (H) Graph of compound fluvial sheet percentage against distance downstream. (I) Overbank contour map. (J) Graph of overbank percentage against distance downstream. Average measurements of proximal, medial and distal portions are denoted as P (av), M (av) and D (av) on each graph. Dashed line in each case is a linear best fit to the total dataset and the dotted line in each case is a linear best fit line excluding the data influenced by the secondary fluvial source.

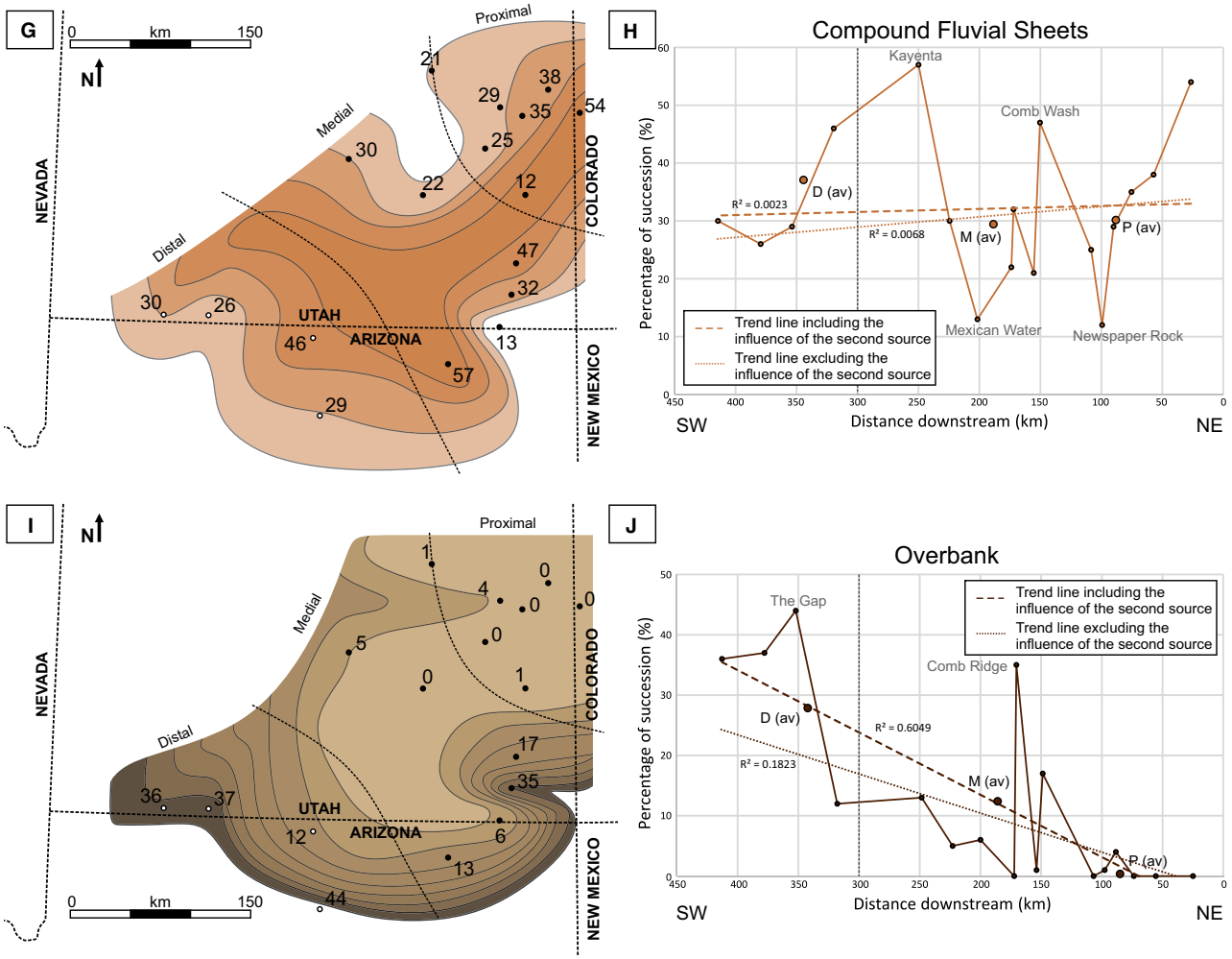

Fig. 7. Continued

15% (The Gap) and 31% (Lees Ferry) by the distal regions.

The relative proportions of isolated sandstone-dominated channel-fill elements gradually increase downstream, although the relationship is weak (Fig. 7C and D). Low proportions of isolated sandstone-dominated channel-fill are preserved within the fluvial sediments of the eastern proximal to medial regions (0% at Sevenmile Canyon and Kayenta, 1% at Newspaper Rock, and 3% at both Comb Ridge and Comb Wash) with slightly higher proportions preserved towards the west/south-west in the medial and distal regions (13% at The Gap, 12% at Hickman Bridge Trail and 11% at Kanab). Despite an apparent overall increase in abundance with distance downstream, the relative proportions of isolated sandstone-dominated channel elements in some proximal and medial areas are somewhat anomalous. For example, at Mexican Water, anomalously high proportions of isolated sandstone-dominated channel-fill elements (35%) may be a result of under-sampling due to the small outcrop. The relatively low gradient of the relationship between the proportions of isolated sandstone-dominated channel-fill elements and the distance downstream (Fig. 7C and D) may suggest that this relationship is controlled primarily by the diminishing abundance of other channel-fill elements with distance downstream, and there is little downstream control on the presence of this depositional element.

Both isolated gravel-dominated channel-fill (Fig. 7E and F) and compound sandstone-dominated fluvial sheet (Fig. 7G and H) depositional

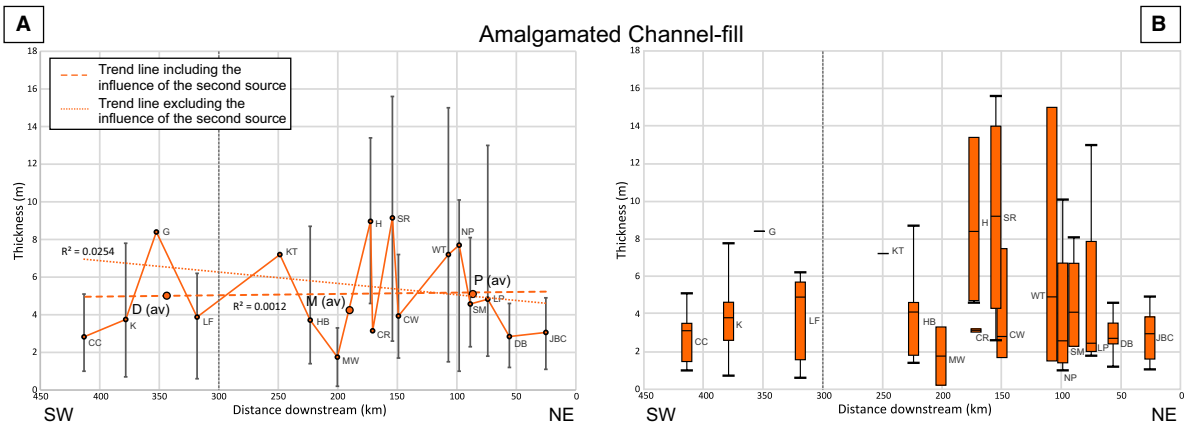

	JBC	DB	LP	SM	NP	WT	CW	SR	CR	H	MW	HB	KT	LF	G	K	CC
n	5	7	4	7	4	3	3	4	2	3	2	7	1	5	1	10	7
av.	3.06	2.84	4.83	4.57	7.70	7.20	3.93	9.15	3.15	8.97	1.75	3.71	7.20	3.88	8.40	3.75	2.83
med.	2.95	2.70	2.45	4.10	2.55	4.90	2.80	9.20	3.15	8.40	1.75	4.10	7.20	4.90	8.40	3.80	3.10
IQR	2.15	1.10	5.85	4.40	5.30	13.5	5.75	9.70	0.10	8.70	3.10	2.80	-	4.15	-	2.00	1.90

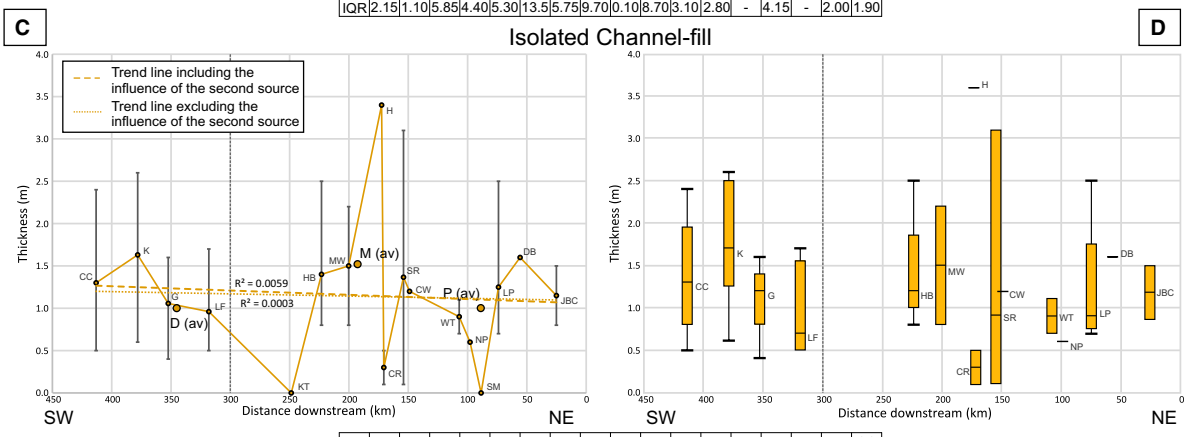

	JBC	DB	LP	SM	NP	WT	CW	SR	CR	H	MW	HB	KT	LF	G	K	CC
n	2	1	4	0	1	2	1	3	2	1	2	4	0	5	7	10	4
av.	1.15	1.60	1.25	-	0.60	0.90	1.20	1.37	0.30	3.40	1.50	1.40	-	0.96	1.06	1.63	1.30
med.	1.18	1.60	0.90	-	0.60	0.90	1.20	0.90	0.30	3.40	1.50	1.20	-	0.70	1.20	1.70	1.30
IQR	0.65	-	1.00	-	-	0.40	-	3.00	0.40	-	1.40	0.85	-	1.05	0.60	1.25	1.15

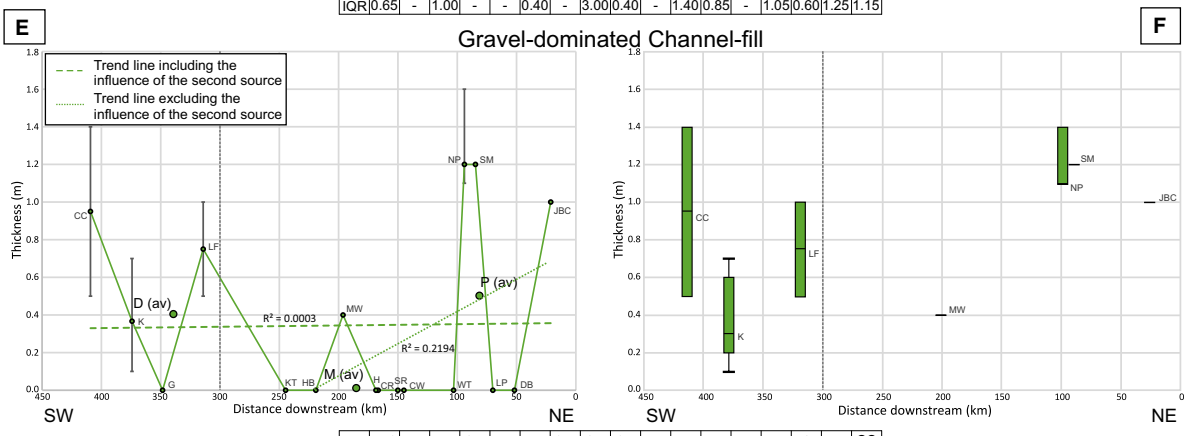

	JBC	DB	LP	SM	NP	WT	CW	SR	CR	H	MW	HB	KT	LF	G	K	CC
n	1	0	0	1	3	0	0	0	0	0	1	0	0	2	0	6	2
av.	1.00	-	-	1.20	1.20	-	-	-	-	-	0.40	-	-	0.75	-	0.37	0.95
med.	1.00	-	-	1.20	1.10	-	-	-	-	-	0.40	-	-	0.75	-	0.30	0.95
IQR	-	-	-	-	0.3	-	-	-	-	-	-	-	-	0.50	-	0.40	0.90

Fig. 8. Graphs illustrating the average and range of sediment thickness at each locality for each depositional element plotted against distance downstream and box and whisker plots illustrating the median, interquartile range and outliers for each locality for each depositional element plotted against distance downstream. Average measurements of proximal, medial and distal portions are denoted as P (av), M (av) and D (av) on each graph. Dashed line in each case is a linear best fit to the total dataset and the dotted line in each case is a linear best fit line excluding the data influenced by the secondary fluvial source.

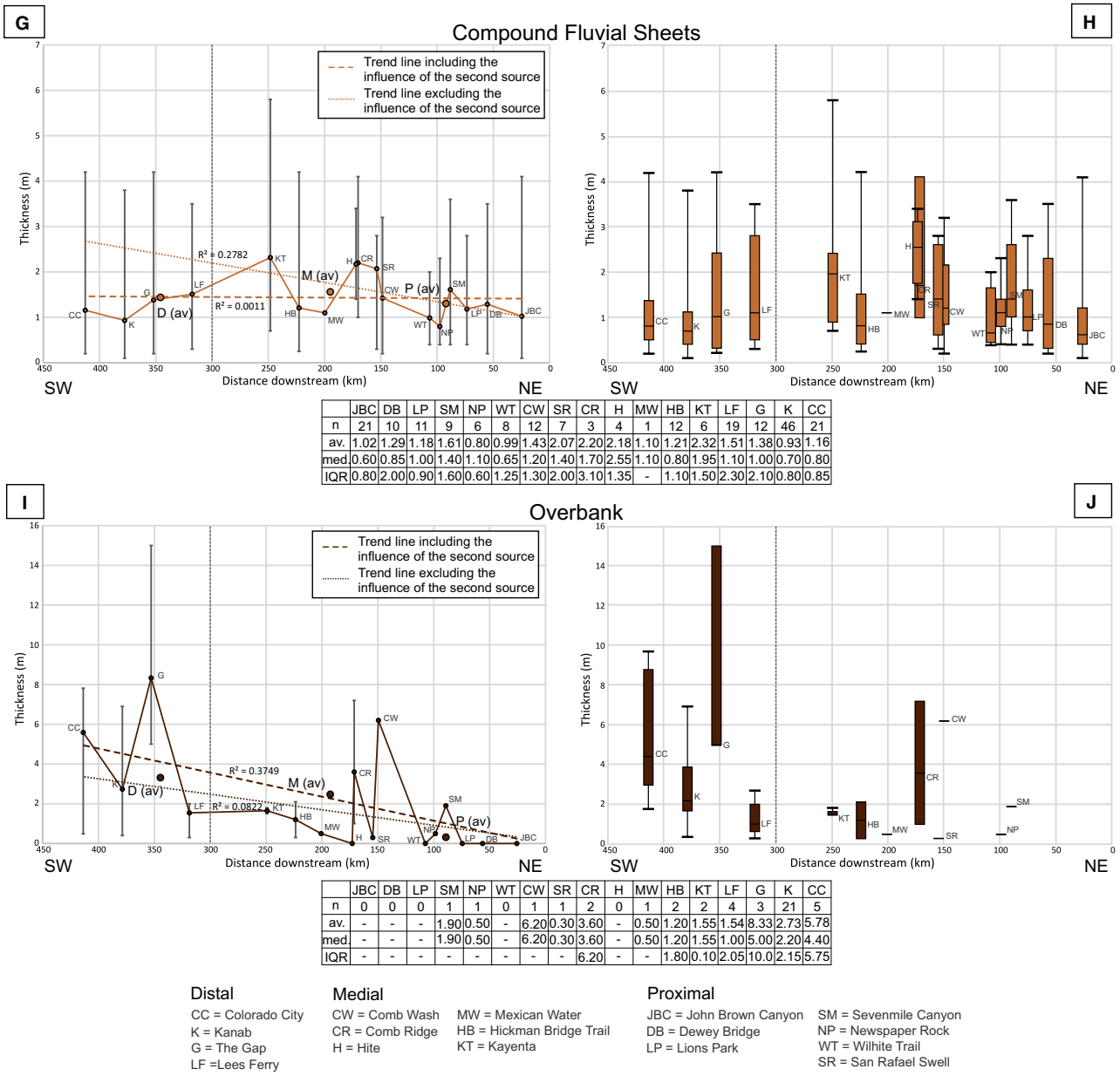

	JBC	DB	LP	SM	NP	WT	CW	SR	CR	H	MW	HB	KT	LF	G	K	CC
n	21	10	11	9	6	8	12	7	3	4	1	12	6	19	12	46	21
av.	1.02	1.29	1.18	1.61	0.80	0.99	1.43	2.07	2.20	2.18	1.10	1.21	2.32	1.51	1.38	0.93	1.16
med	0.60	0.85	1.00	1.40	1.10	0.65	1.20	1.40	1.70	2.55	1.10	0.80	1.95	1.10	1.00	0.70	0.80
IQR	0.80	2.00	0.90	1.60	0.60	1.25	1.30	2.00	3.10	1.35	-	1.10	1.50	2.30	2.10	0.80	0.85

	JBC	DB	LP	SM	NP	WT	CW	SR	CR	H	MW	HB	KT	LF	G	K	CC
n	0	0	0	1	1	0	1	1	2	0	1	2	2	4	3	21	5
av.	-	-	-	1.90	0.50	-	6.20	0.30	3.60	-	0.50	1.20	1.55	1.54	8.33	2.73	5.78
med	-	-	-	1.90	0.50	-	6.20	0.30	3.60	-	0.50	1.20	1.55	1.00	5.00	2.20	4.40
IQR	-	-	-	-	-	-	-	-	6.20	-	-	1.80	0.10	2.05	10.0	2.15	5.75

Distal
CC = Colorado City
K = Kanab
G = The Gap
LF =Lees Ferry

Medial
CW = Comb Wash
CR = Comb Ridge
H = Hite
MW = Mexican Water
HB = Hickman Bridge Trail
KT = Kayenta

Proximal
JBC = John Brown Canyon
DB = Dewey Bridge
LP = Lions Park
SM = Sevenmile Canyon
NP = Newspaper Rock
WT = Wilhite Trail
SR = San Rafael Swell

Fig. 8. Continued

elements display very weak decreasing trends in relative proportions with distance downstream.

Thickness of depositional elements

Weak downstream trends in the average thicknesses of the depositional elements are observed (Fig. 8). The overbank depositional elements (Fig. 8E) and isolated sandstone-dominated channel-fill elements (Fig. 8B) display slight increases in their average thicknesses towards the distal region. Amalgamated sandstone-dominated channel-fill (Fig. 8A), isolated gravel-dominated channel-fill (Fig. 8C) and compound sandstone-dominated fluvial sheet (Fig. 8D) depositional elements all show very little to no variation downstream. However, when the data from elements displaying sediment derived from the secondary fluvial source are removed, a strong downstream trend is observed, with the thickness of isolated gravel-dominated channel-fill elements decreasing with distance downstream (Fig. 8C).

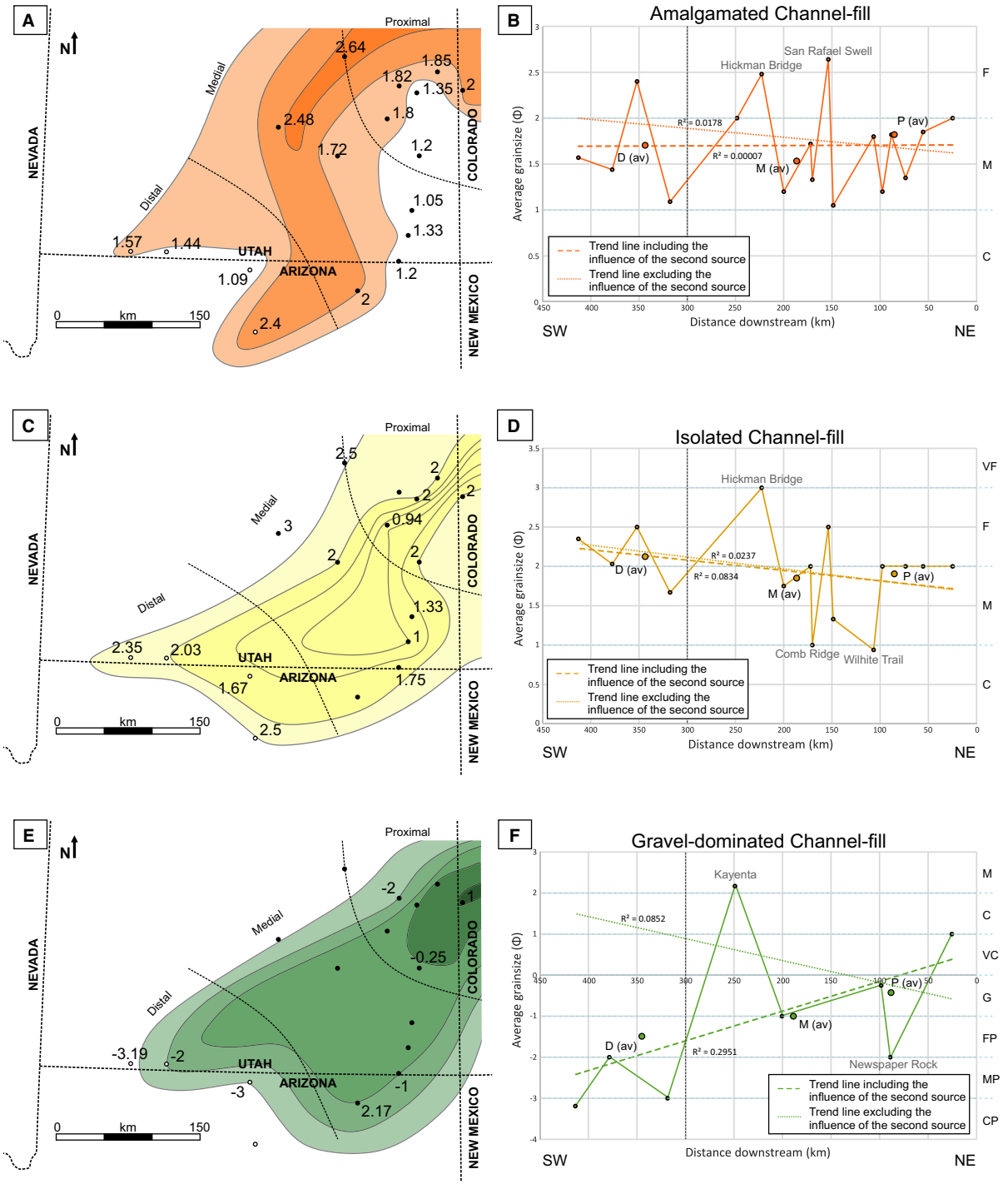

Fig. 9. Contour maps and graphs illustrating the average grain size (*Φ*) that each depositional element constitutes of the fluvial succession at each locality. (A) Amalgamated channel contour map. (B) Graph of amalgamated channel average grain size against distance downstream. (C) Isolated channel contour map. (D) Graph of isolated channel average grain size against distance downstream. (E) Gravel-dominated channel contour map. (F) Graph of gravel-dominated channel average grain size against distance downstream. (G) Compound fluvial sheet contour map. (H) Graph of compound fluvial sheet average grain size against distance downstream. (I) Overbank contour map. (J) Graph of overbank average grain size against distance downstream. Average measurements of proximal, medial and distal portions are denoted as P (av), M (av) and D (av) on each graph. Dashed line in each case is a linear best fit to the total dataset and the dotted line in each case is a linear best fit line excluding the data influenced by the secondary fluvial source.

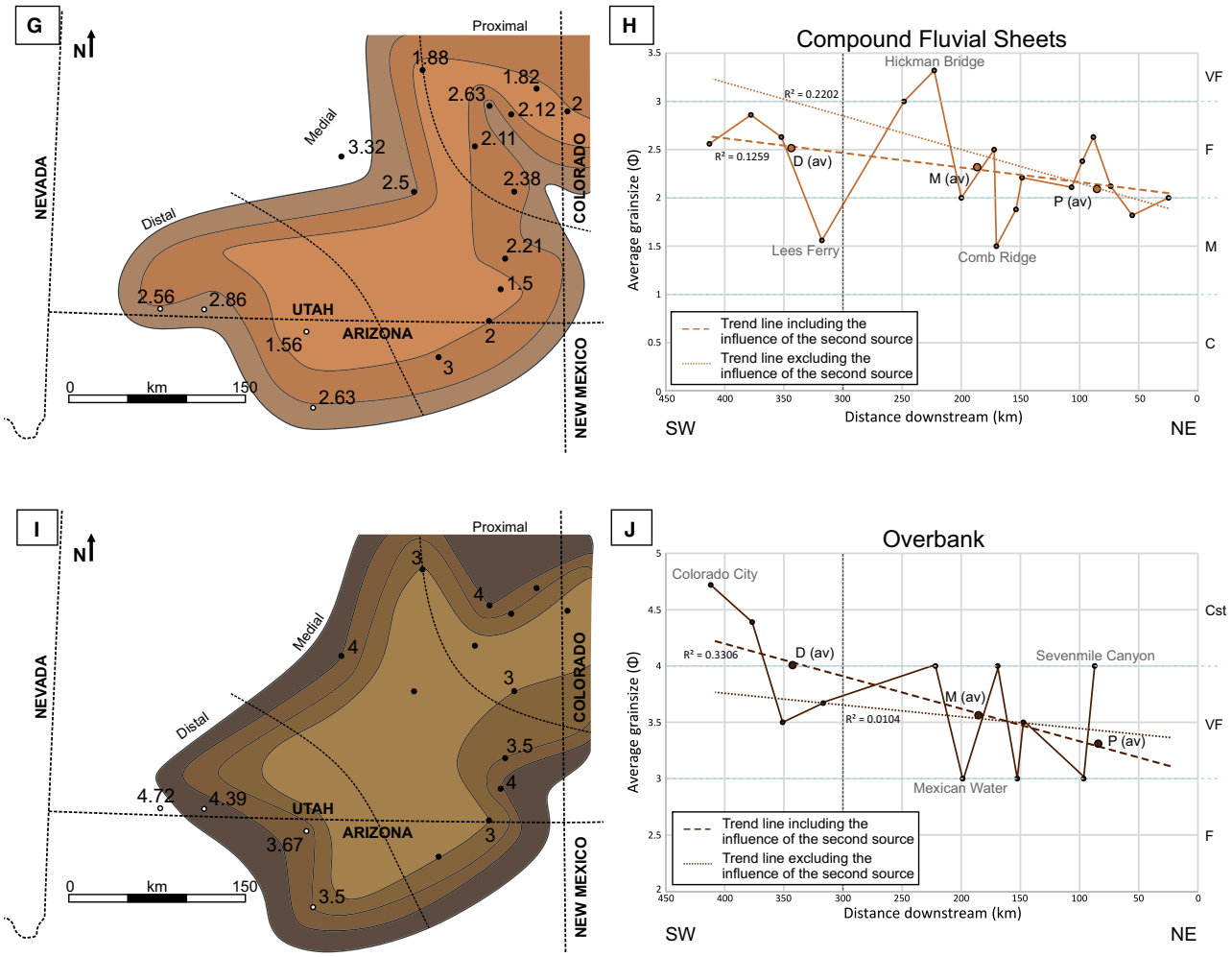

Fig. 9. Continued

Grain-size distribution of the depositional elements

Contrary to the first-order trend that is typical of all fluvial systems, the amalgamated sandstone-dominated channel-fill depositional element shows no downstream decrease in grain size (Fig. 9A and B). Sediment calibre is consistently medium-grained sandstone throughout most of the system, although a few locations in the proximal and medial regions preserve anomalously finer grained fluvial sediment (San Rafael Swell – 2.64ϕ and Hickman Bridge Trail – 2.48ϕ). However, once data from elements displaying sediment derived from the secondary fluvial source are removed, a weak trend is observed, with a decrease in grain size with distance downstream (Fig. 9A and B). Isolated sandstone-dominated channel-fill elements have a very weak downstream trend, displaying a gradual decrease in grain size, from medium-grained sandstone within the proximal to fine-grained sandstone within the distal (Fig. 9C and D). The isolated gravel-dominated channel-fill depositional element has a strong downstream trend, but not in the manner that could be intuitively predicted (Fig. 9E and F). An increase in grain size with distance downstream is observed, from very coarse-grained sandstone within the proximal to medium to coarse-grained pebbles within the distal. However, once data from elements displaying sediment derived from the secondary fluvial source are removed, a strong decrease in grain size with distance downstream is observed, from a granule-grade conglomerate in the proximal to a coarse-grained sandstone in the distal. Compound sandstone-dominated fluvial sheet

elements have a very weak downstream trend, displaying a gradual decrease in grain size, from medium-grained sandstone within the proximal region to fine-grained sandstone within the distal region (Fig. 9G and H). However, once the data from elements displaying sediment derived from the secondary fluvial source are removed, a strong downstream trend is observed, with a decrease in grain size from medium-grained sandstone within the proximal region to very fine-grained sandstone within the distal region (Fig. 9G and H). The overbank depositional element has the strongest trend, with an overall decrease in grain size with distance downstream, from fine to very fine-grained sandstone within the proximal to coarse siltstone within the distal (Fig. 9I and J).

INTERPRETATION AND DISCUSSION

Spatial variations in the sedimentology of the Kayenta Formation

The high degree of channel and sheet amalgamation and connectivity within proximal region suggests that the fluvial system was highly cannibalistic (North & Taylor, 1996; Hassan *et al.*, 2018; Priddy & Clarke, 2020) with a high sediment supply (Weissmann *et al.*, 2013; Owen *et al.*, 2015). The decrease in channel and sheet amalgamation, increase in the proportion of overbank, and overall grain-size reduction downstream can be attributed to a downstream decrease in energy and a downstream decrease in the river's carrying capacity as a result of lateral expansion of the river system, channel bifurcation and high rates of evapotranspiration and infiltration into the dry substrate (Nichols & Fisher, 2007; Weissmann *et al.*, 2010, 2013; Sutfin *et al.*, 2014; Owen *et al.*, 2015) (Fig. 10). The abundance of preserved channel depositional elements within the distal region may also be the result of preferential preservation and the function of channel belt avulsion, resulting in the preservation of channel elements at the same stratigraphic level that are not time equivalent (North & Warwick, 2007).

However, it must be noted that a decrease in amalgamation of channel and compound sheet elements, coupled with an overall increase in the total fluvial sediment thickness observed at each locality, could also be attributed to increased subsidence and the generation of additional accommodation space, coevally with deposition of the Kayenta sediments, as in the distal region where deposition of the Kayenta correlates with the location of the Zuni Sag (Fig. 1) (Blakey, 1994). It is also possible that the increase in cumulative fluvial sediment thickness within the distal section may also be attributed to a secondary, axial fluvial system, sourced from the Mogollon Highlands in the Cordilleran Magmatic Arc (Luttrell, 1993; Hassan *et al.*, 2018) feeding additional sediment volume into the Zuni Sag, although ultimately the thickness of sediment preserved is probably controlled by developing accommodation space over any other factor.

Spatial variations in depositional elements

Amalgamated sandstone-dominated channel-fill depositional elements display downstream fluvial trends typical of fluvial systems including a decrease in their abundance and decrease in their constituent grain size downstream. They can be attributed to a decrease in energy downstream as a result of high rates of evapotranspiration and infiltration into the dry substrate and channel bifurcation (Nichols & Fisher, 2007; Weissmann *et al.*, 2010, 2013; Sutfin *et al.*, 2014; Owen *et al.*, 2015) or avulsion of the channel belt (North & Warwick, 2007).

A relatively flat linear trend line for the percentage of isolated sandstone-dominated channel-fill depositional elements suggests that there is no downstream control on the presence of this element. The very slightly higher prevalence in this element downstream that the data suggest is of little significance and may be due simply to the diminishing abundance of other channel-fill elements downstream. The increase in the average thicknesses of the isolated sandstone-dominated channel-fill depositional elements downstream is probably the result of increased preservation potential within the distal setting, where full thicknesses of the isolated channels are more likely to be preserved.

Isolated gravel-dominated channel-fill depositional elements comprise only a small proportion of the fluvial succession with distance downstream. However, the grain size of the isolated gravel-dominated channel-fill depositional elements increases downstream; a trend that is contrary to that intuitively expected for any waning fluvial system. This observation may be due directly to the secondary source of coarse-grained Kayenta fluvial sediment in south-west Utah (Luttrell, 1993) and it is something that

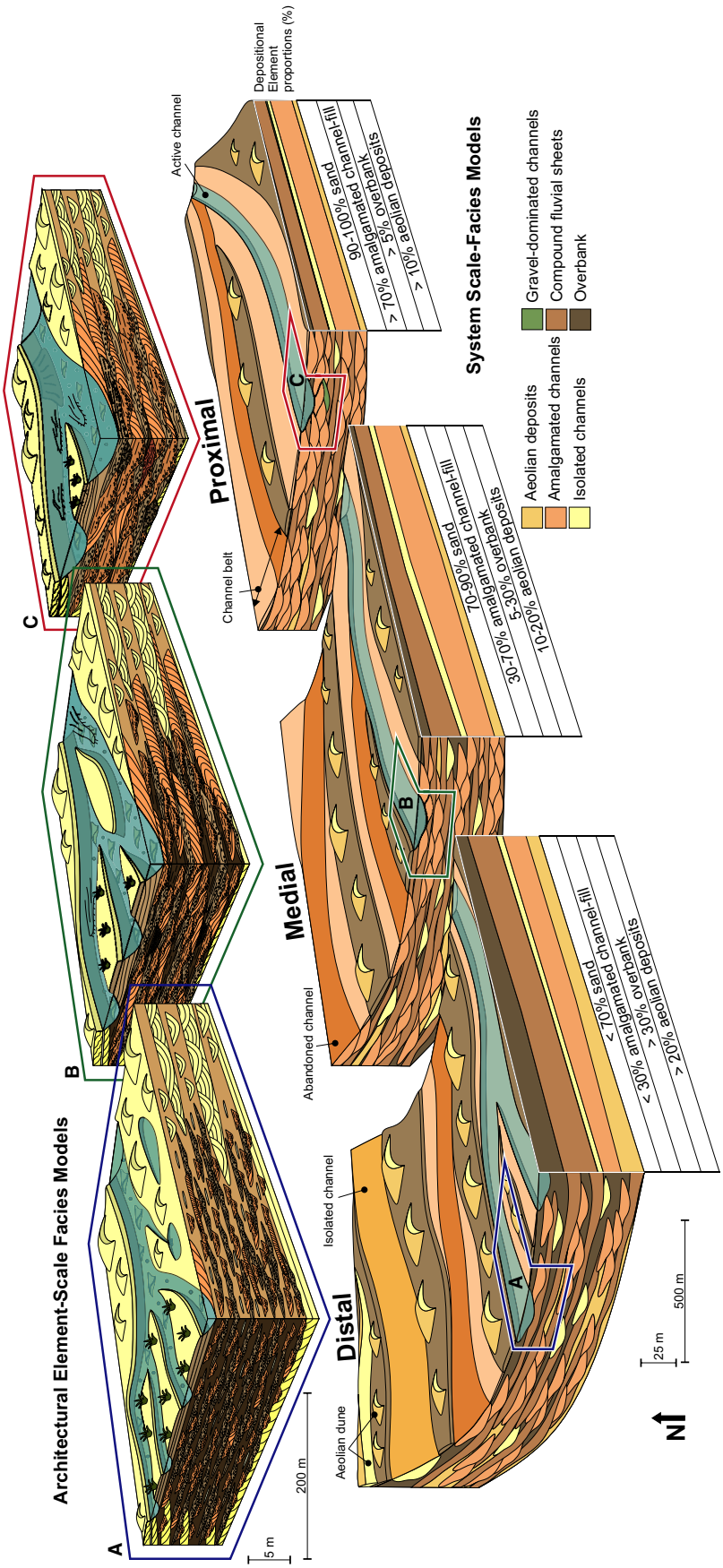

Fig. 10. System-scale depositional model of the Kayenta Formation sub-divided into proximal, medial and distal sections with a cross-section of the internal architecture and stacking patterns for each section. Depositional element proportions (%) are displayed along the side of each section of the system-scale model, along with their key characteristics. Architectural element-scale facies models of the proximal, medial and distal settings highlight the detailed sedimentology observed within the depositional elements on the system-scale model.

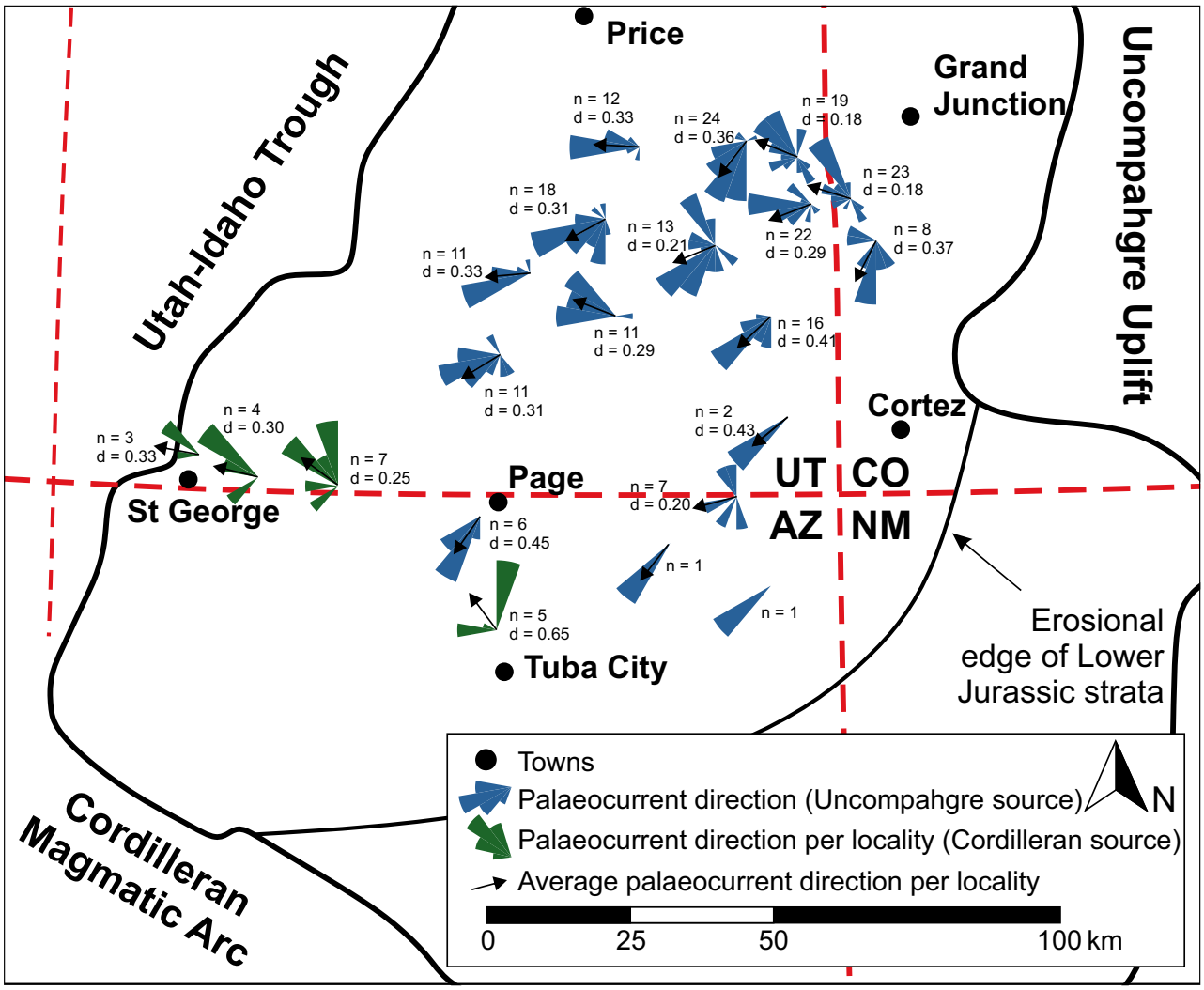

Fig. 11. Palaeocurrent measurements of the fluvial sediment at each locality depicted by rose diagrams coloured by sediment source. The black arrows indicate the average palaeocurrent direction per locality along with the number of measurements and degree of dispersion per locality.

would require in-depth petrographical and provenance studies to examine further.

Analysis of the compound sandstone-dominated fluvial sheet depositional elements reveal relatively constant percentage of elements and average thicknesses downstream. The flat linear trend lines for these characteristics suggests that there is no downstream control on the presence of this element, and the occasional more prevalent appearance downstream may be due to the interaction with the secondary fluvial system within the distal region.

The overbank depositional elements display the strongest trends within the data; an increase in the percentage and thickness of overbank downstream and a decrease in grain size downstream, all of which are typical for a waning fluvial system. These trends are a result of the decrease in energy and the river's carrying capacity downstream as a result of lateral expansion of the river system, channel bifurcation and high rates of evapotranspiration and infiltration into the dry substrate (Nichols & Fisher, 2007; Weissmann *et al.*, 2010, 2013; Sutfin *et al.*, 2014; Owen *et al.*, 2015) or avulsion of the channel belt (North & Warwick, 2007).

The sand-dominated fluvial depositional elements (amalgamated channel, isolated channel and compound sheet elements) display no significant trends in grain-size distribution downstream. Each of these elements is dominated by fine to medium-grained sandstone of aeolian origin that has been blown off coeval dune fields, reworked

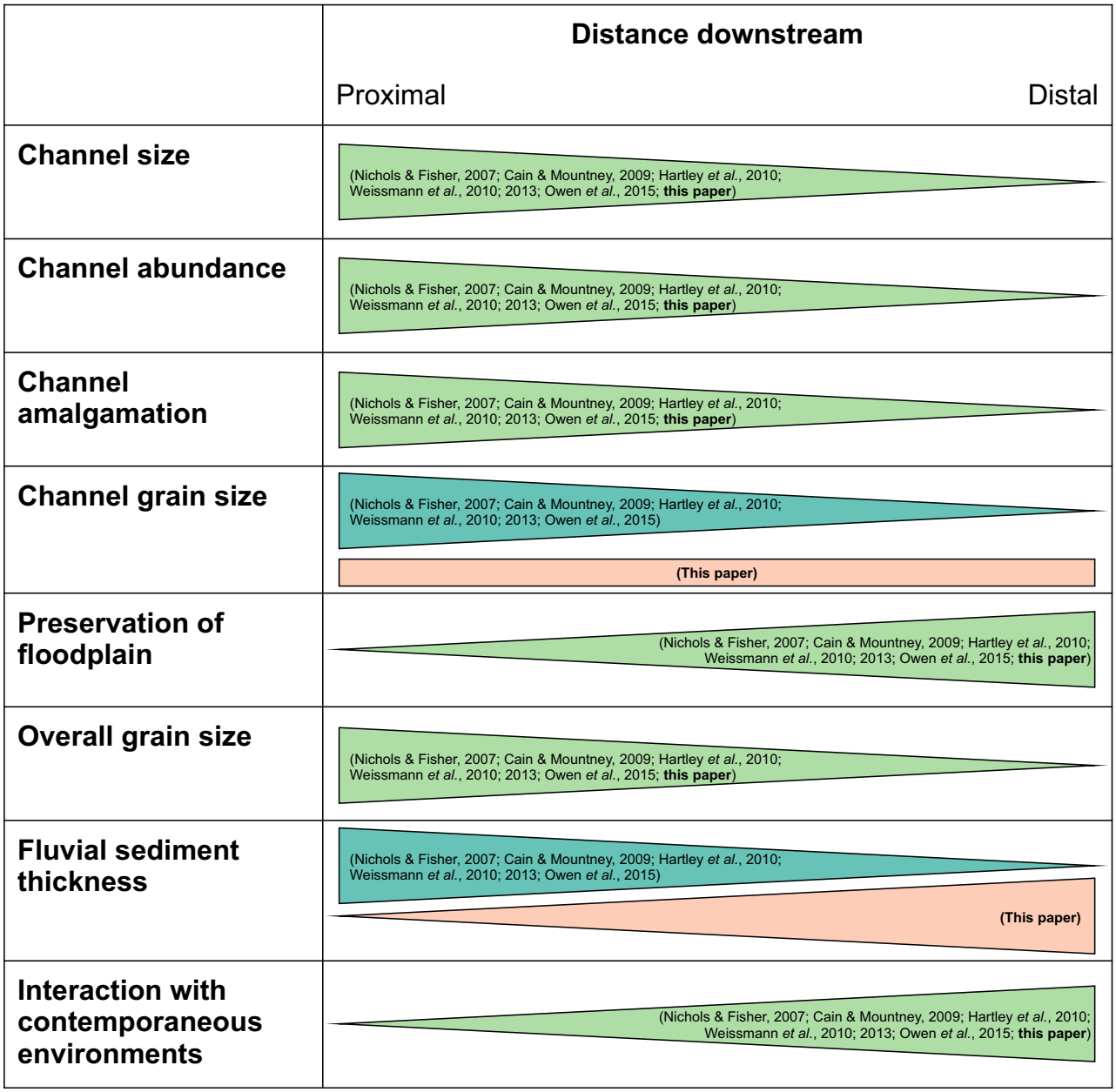

Fig. 12. Comparison of key characteristics of a distributive fluvial system. Triangles represent whether a key characteristic increases or decreases downstream and are coloured by similarities and differences in findings from previously published literature.

and transported by the fluvial system (Priddy & Clarke, 2020). Coeval aeolian systems are a typical feature of many modern arid ephemeral fluvial basins (Veiga *et al.*, 2002; Al-Masrahy & Mountney, 2015; Formolo Ferronatto *et al.*, 2019; Reis *et al.*, 2019; Coronel *et al.*, 2020) and many preserved examples of arid fluvial strata contain significant proportions of aeolian sediment (Langford, 1989; Clarke & Rendell, 1998; Bullard & Livingstone, 2002; Field *et al.*, 2009). This relationship could be recognized as a characteristic of dryland ephemeral fluvial systems.

Comparison to distributive fluvial system models

Analysis of the downstream trends of the dryland ephemeral fluvial Kayenta Formation

illustrates a number of characteristics that are similar to those displayed by typical terminal fluvial fans and some distributive fluvial systems described by Hampton & Horton (2007), Nichols & Fisher (2007), Fisher *et al.* (2008), Cain & Mountney (2009), Hartley *et al.* (2010), Weissmann *et al.* (2010, 2013) and Owen *et al.* (2015). The Kayenta fluvial sediments display a clear lack of confinement of the fluvial system sourced from the Uncompahgre Uplift, illustrating very little evidence of significant tributary inputs, until the intersection with the axial fluvial system sourced from the Cordilleran Magmatic Arc (Fig. 11). A downstream decrease in amalgamation of channels and compound sheets (Fig. 3), a small decrease in grain size downstream (Fig. 6I and J) and an overall increase in the percentage of overbank depositional elements with distance downstream (Fig. 7I and J) are also observed, all of which are characteristics that are consistent with previously published models (Nichols & Fisher, 2007; Hartley *et al.*, 2010; Weissmann *et al.*, 2010, 2013; Owen *et al.*, 2015) (Fig. 12). Consequently, a downstream decrease in both energy and channel bifurcation, accompanied by high rates of evapotranspiration and infiltration of water into the substrate are considered the probable mechanisms that explain these trends in the Kayenta ephemeral fluvial sediments, just as they do in these models (Nichols & Fisher, 2007; Weissmann *et al.*, 2010, 2013; Sutfin *et al.*, 2014).

Conversely, there are several downstream relationships displayed by the Kayenta fluvial sediments that do not fit with published models. In the Kayenta, the total thicknesses of the fluvial sediment increase with distance downstream, the thicknesses of the channel-fill and sheet depositional elements display no significant relationships to distance downstream, and the channel-fill depositional elements downstream display no significant variation in average grain size with distance downstream (*cf:* Friend & Moody-Stuart, 1972; Friend, 1978; Nichols, 1987; Hirst, 1991; Stanistreet & McCarthy, 1993; Nichols & Fisher, 2007; Cain & Mountney, 2009; Hartley *et al.*, 2010; Weissmann *et al.*, 2010, 2013; Owen *et al.*, 2015) (Fig. 11).

Some of these anomalous trends may be attributable to case-specific external factors – an increase in total thicknesses of fluvial sediment downstream may be attributed to the increase in accommodation space provided by the Zuni Sag and Utah-Idaho Trough (Blakey, 2008), and relatively constant thicknesses of channel-fill and sheet depositional elements with distance downstream may be attributed to the influence of the secondary fluvial source (Luttrell, 1993) – but, equally, external factors do not explain characteristics such as the channel-fill depositional elements that display no significant variation in average grain size with distance downstream. This relationship may be the consequence of the interaction between a fluvial system and an ever-present coeval aeolian system throughout the fluvial course. Significant volumes of sediment derived locally from the aeolian system and fluvially reworked, may limit the downstream grain-size distribution of the fluvial deposits. Given that dryland ephemeral fluvial systems are typified by their close spatial and temporal links to aeolian systems, it is possible that some of these trends are typical of dryland ephemeral fluvial systems in general, but significant studies of comparative dryland systems are required to confirm such.

CONCLUSIONS

The spatial distribution and downstream trends of the Lower Jurassic Kayenta Formation of south-western USA, have been examined quantitatively and the analysis reveals a number of downstream trends in this ancient dryland ephemeral system. Some trends are similar to those observed in previously published distributive fluvial system (DFS) models, including; a lack of confinement of the fluvial system, a downstream decrease in channel and sheet architectural element amalgamation, a downstream decrease in grain size, albeit very small, a downstream decrease in preserved channel and sheet width-to-thickness ratios, and an increase in the percentage of overbank elements downstream. Consequently, these trends may be attributed to the same controlling factors as those attributed to published models. However, other relationships do not match the DFS model. While some of these relationships may be explained by the influence of external factors inherent in this study, others, including the channel-fill depositional elements that display no significant variation in average grain size with distance downstream, may be a consequence of fluvial interaction with a competing and coeval aeolian system. Given that dryland ephemeral fluvial systems are typified by their

close spatial and temporal links to aeolian systems, these trends may be typical of dryland ephemeral fluvial systems in general, although the single study presented in this work is an insufficient dataset to determine this.

The analyses presented here demonstrate the inherent complexity in arid dryland fluvial systems and the downstream architectural and compositional relationships that they depict. This complexity arises not only from the style of the fluvial system and the climatic regime under which it evolves, but also from basinal factors and from the interaction with coeval environments. Consequently, models for fluvial style provide a good first-order approximation for architectural and compositional downstream trends in arid dryland systems, but the detail is strongly dependent upon external setting and internal complexity. This study highlights these important differences, and it reveals some of the value in applying generic fluvial models to the interpretation of subsurface data for resource exploitation, but the study also highlights the great dangers in over reliance on such an approach, particularly in arid dryland systems. The controlling factors upon these systems are inherently difficult to unravel. Consequently, a generalized model may not always be applicable.

ACKNOWLEDGEMENTS

This research was conducted during a study undertaken as part of the Natural Environment Research Council (NERC) Centre for Doctoral Training (CDT) in Oil & Gas under its Extending the Life of Mature Basins theme [grant number: NEM00578X/1]. It is sponsored by NERC and the British Geological Survey (BGS) via the British University Funding Initiative (BUFI) whose support is gratefully acknowledged. We are also grateful to the United States National Park Service for permitting this research and granting scientific research permits for Arches, Canyonlands, Capitol Reef and Zion National Parks, and to the Navajo Nation for granting access to conduct research within their land. Ross Pettigrew, David Cousins and Andrew Mitten are acknowledged for providing valuable field support and assisting with observations and interpretations. We are very grateful to Nigel Mountney, Colin North, Jonathan Redfern and one anonymous reviewer for their constructive and extremely useful comments that have greatly improved this work. The authors declare that they have no conflict of interests and the data that support the findings of this study are available from the corresponding author upon reasonable request.

REFERENCES

Aliyuda, K. and **Howell, J.** (2021) Progradation of a mid-Cretaceous distributive fluvial system: The upper member of the Bima Formation, Northern Benue Trough, Nigeria. *Sedimentology*, **68**, 1861–1876.

Allen, J.R.L. (1974) Studies in fluviatile sedimentation: Implications of pedogenic carbonate units. Lower Old Red Sandstone, Anglo-Welsh outcrop. *Geol. J.*, **9**(2), 181–208.

Allen, J.R.L. and **Banks, N.L.** (1972) An interpretation and analysis of recumbent-folded deformed cross-bedding. *Sedimentology*, **19**(3–4), 257–283.

Al-Masrahy, M.A. and **Mountney, N.P.** (2015) A classification scheme for fluvial–aeolian system interaction in desert-margin settings. *Aeol. Res.*, **17**, 67–88.

Babcock, H.M. and **Cushing, E.M.** (1941) Recharge to ground water from floods in a typical desert wash, Pinal County, Arizona. *Eos Trans. AGU*, **23**, 49–56.

Bachmann, G.H. and **Wang, Y.** (2014) Armoured mud balls as a result of ephemeral fluvial flood in a humid climate: Modern example from Guizhou Province, South China. *J Palaeogeogr*, **3**(4), 410–418.

Billi, P., **Demissie, B.**, **Nyssen, J.**, **Moges, G.** and **Fazzini, M.** (2018) Meander hydromorphology of ephemeral streams: similarities and differences with perennial rivers. *Geomorphology*, **319**, 35–46.

Bjerrum, C.J. and **Dorsey, R.J.** (1995) Tectonic Controls on deposition of Middle Jurassic strata in a retroarc foreland basin, Utah-Idaho trough, western interior, United States. *Tectonics*, **14**(4), 962–978.

Blakey, R.C. (1994) Paleogeographic and tectonic controls on some Lower and Middle Jurassic erg deposits, Colorado Plateau. In: *Mesozoic Systems of the Rocky Mountain Region, USA* (Eds Caputo, M.V., Peterson, J.A., Franczyk, K.J.), pp. 273–298.Rocky Mountain Section (SEPM), Denver.

Blakey, R.C. (2008) Pennsylvanian–Jurassic sedimentary basins of the Colorado Plateau and southern Rocky Mountains. In: *Sedimentary Basins of the United States and Canada*, **5** (Ed. Miall, A.D.), 1st edn., pp. 245–296. Elsevier, Amsterdam, The Netherlands.

Blakey, R. and **Ranney, W.** (2018) *Ancient Landscapes of Western North America: A Geologic History with Paleogeographic Maps*, 1st edn. Springer, Cham, Switzerland, 234 pp.

Bridge, J.S. (2003) *Rivers and Floodplains: Forms, Processes, and Sedimentary Record*. Blackwell Scientific Publishing, Oxford, 491 pp.

Bridge, J.S. (2006) Fluvial facies models: recent developments. In: *Facies Models Revisited* (Eds Posamentier, H.W. and Walker, R.G.), *SEPM Special Publication*, **84**, 85–170.

Bridge, J.S. and **Best, J.L.** (1988) Flow, sediment transport and bedform dynamics over the transition from dunes to upper-stage plane beds: implications for the formation of planar laminae. *Sedimentology*, **35**(5), 753–763.

Bromley, M.H. (1991) Architectural features of the Kayenta Formation (Lower Jurassic), Colorado Plateau, USA:

relationship to salt tectonics in the Paradox Basin. *Sed. Geol.*, **73**(1–2), 77–99.

Bullard, J.E. and **Livingstone, I.** (2002) Interactions between aeolian and fluvial systems in dryland environments. *Area*, **34**(1), 8–16.

Cain, S.A. and **Mountney, N.P.** (2009) Spatial and temporal evolution of a terminal fluvial fan system: the Permian Organ Rock Formation, South-east Utah, USA. *Sedimentology*, **56**(6), 1774–1800.

Cain, S.A. and **Mountney, N.P.** (2011) Downstream changes and associated fluvial-aeolian interactions in an ancient terminal fluvial fan system: the Permian Organ Rock Formation, SE Utah. In: *From River to Rock Record* (Eds Davidson, S., Leleu, S. and North, C.), *SEPM Special Publication*, **97**, 165–187.

Carpenter, M.C. and **Morales, M.** (1996) Synopsis of the Kayenta Formation. In: *Guidebook for the Geological Excursion of the Continental Jurassic Symposium: Flagstaff, Museum of Northern Arizona* (Ed. Morales, M.), pp. 15–23. Museum of Northern Arizona Press, Flagstaff, AZ.

Chidsey Jr, T.C. (2013) Geology of the San Rafael Swell, east-central Utah. In: *The San Rafael Swell and Henry Mountains Basin–Geologic Centerpiece of Utah: Salt Lake City* (Eds Morris, T.H. and Ressetar, R.), *Utah Geological Association Publication*, **42**, 1–74.

Clarke, M.L. and **Rendell, H.M.** (1998) Climate change impacts on sand supply and the formation of desert sand dunes in the south-west USA. *J Arid Environ*, **39**(3), 517–531.

Colombera, L., **Mountney, N.P.** and **McCaffrey, W.D.** (2013) A quantitative approach to fluvial facies models: Methods and example results. *Sedimentology*, **60**(6), 1526–1558.

Colombera, L. and **Mountney, N.P.** (2019) The lithofacies organization of fluvial channel deposits: A meta-analysis of modern rivers. *Sed. Geol.*, **383**, 16–40.

Cornish, J.H. (1961) Flow losses in dry sandy channels. *J. Geophys. Res.*, **66**(6), 1845–1853.

Coronel, M.D., **Isla, M.F.**, **Veiga, G.D.**, **Mountney, N.P.** and **Colombera, L.** (2020) Anatomy and facies distribution of terminal lobes in ephemeral fluvial successions: Jurassic Tordillo Formation, Neuquén Basin, Argentina. *Sedimentology*, **67**(5), 2596–2624.

Davidson, S., **Hartley, A.J.**, **Weissmann, G.S.**, **Nichols, G.J.** and **Scuderi, L.A.** (2013) Geomorphic elements on modern distributive fluvial systems. *Geomorphology*, **180–181**, 82–95.

Dickinson, W.R. (2018) *Tectonosedimentary Relations of Pennsylvanian to Jurassic Strata on the Colorado Plateau*. (Vol. **533**). Special Paper. Geological Society of America, Boulder, CO, 184 pp.

Field, J.P., **Breshears, D.D.** and **Whicker, J.J.** (2009) Toward a more holistic perspective of soil erosion: why aeolian research needs to explicitly consider fluvial processes and interactions. *Aeol. Res.*, **1**(1–2), 9–17.

Fielding, C.R. (2006) Upper flow regime sheets, lenses and scour fills: extending the range of architectural elements for fluvial sediment bodies. *Sed. Geol.*, **190**(1–4), 227–240.

Fielding, C.R., **Alexander, J.** and **Allen, J.P.** (2018) The role of discharge variability in the formation and preservation of alluvial sediment bodies. *Sed. Geol.*, **365**, 1–20.

Fisher, J.A., **Krapf, C.B.**, **Lang, S.C.**, **Nichols, G.J.** and **Payenberg, T.H.** (2008) Sedimentology and architecture of the Douglas Creek terminal splay, Lake Eyre, central Australia. *Sedimentology*, **55**(6), 1915–1930.

Fisher, J.A., **Nichols, G.J.** and **Waltham, D.A.** (2007) Unconfined flow deposits in distal sectors of fluvial distributary systems: examples from the Miocene Luna and Huesca Systems, northern Spain. *Sed. Geol.*, **195**(1–2), 55–73.

Foley, M.G. (1978) Scour and fill in steep, sand-bed ephemeral streams. *Geol. Soc. Am. Bull.*, **89**(4), 559–570.

Formolo Ferronatto, J.P., **dos Santos Scherer, C.M.**, **de Souza, E.G.**, **dos Reis, A.D.** and **de Mello, R.G.** (2019) Genetic units and facies architecture of a Lower Cretaceous fluvial-aeolian succession, São Sebastião Formation, Jatobá Basin, Brazil. *J. S. Am. Earth Sci.*, **89**, 158–172.

Friend, P.F. (1978) Distinctive features of some ancient river systems. In: *Fluvial Sedimentology* (Ed. Miall, A.D.), *Canadian Society of Petroleum Geologists Memoir*, **5**, 531–542.

Friend, P.F. and **Moody-Stuart, M.** (1972) Sedimentation of the Wood Bay Formation (Devonian) of Spitsbergen: regional analysis of a late orogenic basin. *Nor. Polarinst. Skr.*, **157**, 1–77.

Friend, P.F., **Slater, M.J.** and **Williams, R.C.** (1979) Vertical and lateral building of river sandstone bodies, Ebro Basin, Spain. *J. Geol. Soc.*, **136**(1), 39–46.

Geehan, G. and **Underwood, J.** (1993) The use of length distributions in geological modeling. In: *The Geologic Modelling of Hydrocarbon Reservoirs and Outcrop Analogs* (Eds Flint, S.S. and Bryant, I.D.), *Int. Assoc. Sedimentol. Spec. Publ.*, **15**, 205–212.

Gibling, M.R. (2006) Width and thickness of fluvial channel bodies and valley fills in the geological record: a literature compilation and classification. *J. Sediment. Res.*, **76**(5), 731–770.

Gómez-Gras, D. and **Alonso-Zarza, A.M.** (2003) Reworked calcretes: their significance in the reconstruction of alluvial sequences (Permian and Triassic, Minorca, Balearic Islands, Spain). *Sed. Geol.*, **158**(3–4), 299–319.

Gulliford, A.R., **Flint, S.S.** and **Hodgson, D.M.** (2014) Testing applicability of models of distributive fluvial systems or trunk rivers in ephemeral systems: reconstructing 3-D fluvial architecture in the Beaufort Group, South Africa. *J. Sediment. Res.*, **84**(12), 1147–1169.

Hampton, B.A. and **Horton, B.K.** (2007) Sheetflow fluvial processes in a rapidly subsiding basin, Altiplano plateau, Bolivia. *Sedimentology*, **54**(5), 1121–1148.

Harshbarger, J.W., **Repenning, C.A.** and **Irwin, J.H.** (1957) Stratigraphy of the uppermost Triassic and the Jurassic rocks of the Navajo Country (Colorado Plateau). *Prof. Paper. US Geol. Survey*, **291**, 74.

Hartley, A.J., **Weissmann, G.S.**, **Nichols, G.J.** and **Warwick, G.L.** (2010) Large distributive fluvial systems: characteristics, distribution, and controls on development. *J. Sediment. Res.*, **80**(2), 167–183.

Hassan, M.S., **Venetikidis, A.**, **Bryant, G.** and **Miall, A.D.** (2018) The sedimentology of an ERG margin: The Kayenta-Navajo Transition (Lower Jurassic), Kanab, Utah, USA. *J. Sediment. Res.*, **88**(5), 613–640.

Hirst, J.P.P. (1991) Variations in alluvial architecture across the Oligo-Miocene Huesca fluvial system, Ebro Basin, Spain. In: *The Three Dimensional Facies Architecture of Terrigenous Clastic Sediments and Its Implications for Hydrocarbon Discovery and Recovery* (Eds Miall, A.D. and Tyer, N.), *SEPM Concepts in Sedimentology and Paleontology*, **3**, 111–121.

Hooke, J.M. (2016) Morphological impacts of flow events of varying magnitude on ephemeral channels in a semiarid region. *Geomorphology*, **252**, 128–143.

Horn, B.L.D., **Goldberg, K.** and **Schultz, C.L.** (2018) Interpretation of massive sandstones in ephemeral fluvial

settings: A case study from the Upper Candelária Sequence (Upper Triassic, Paraná Basin, Brazil). *J. S. Am. Earth Sci*, **81**, 108–121.

Horton, B.K. and **DeCelles, P.G.** (2001) Modern and ancient fluvial megafans in the foreland basin system of the central Andes, southern Bolivia: implications for drainage network evolution in foldthrust belts. *Basin Res.*, **13**(1), 43–63.

Hunter, R.E. (1977) Basic types of stratification in small eolian dunes. *Sedimentology*, **24**(3), 361–387.

Jaeger, K.L., **Sutfin, N.A.**, **Tooth, S.**, **Michaelides, K.** and **Singer, M.** (2017) Geomorphology and sediment regimes of intermittent rivers and ephemeral streams. In: *Intermittent Rivers and Ephemeral Streams Ecology and Management* (Eds Datry, T., Bonada, N. and Boulton, A.), pp. 21–49. Academic Press, Elsevier, London.

Karcz, I. (1972) Sedimentary structures formed by flash floods in southern Israel. *Sed. Geol*, **7**(3), 161–182.

Kelly, S.B. and **Olsen, H.** (1993) Terminal fans—a review with reference to Devonian examples. *Sed. Geol.*, **85**(1–4), 339–374.

Kirkland, J.I., **Milner, A.R.C.**, **Olsen, P.E.** and **Hargrave, J.E.** (2014) The Whitmore Point Member of the Moenave Formation in its type area in Northern Arizona and its age and correlation with the section in St. George, Utah: evidence for two major lacustrine sequences. In: *Geology of Utah's Far South* (Eds MacLean, J.S., Biek, R.F. and Huntoon, J.E.), *Utah Geological Association Publication*, **43**, 321–355.

Kocurek, G. (1991) Interpretation of ancient eolian sand dunes. *Annu. Rev. Earth Planet Sci.*, **19**(1), 43–75.

Lane, L.J., **Diskin, M.H.** and **Renard, K.G.** (1971) Input-output relationships for an ephemeral stream channel system. *J. Hydrol.*, **13**, 22–40.

Langford, R.P. (1989) Fluvial-aeolian interactions: Part I, modern systems. *Sedimentology*, **36**(6), 1023–1035.

Langford, R.P. and **Chan, M.A.** (1989) Fluvial-aeolian interactions: Part II, ancient systems. *Sedimentology*, **36**(6), 1037–1051.

Long, D.F.G. (2002) Aspects of Late Paleoproterozoic fluvial style: The Uairen Formation, Roraima Supergroup, Venezuela. *Precambrian Sedimentary Environments* (Eds Altermann, W. and Corcoran, P.L.), *Spec. Publ. Int. Ass. Sed.*, **33**, 323–338.

Long, D.F.G. (2006) Architecture of pre-vegetation sandybraided perennial and ephemeral river deposits in Paleoproterozoic Athabasca Group, northern Saskatchewan, Canada as indicators of Precambrian fluvial style. *Sed. Geol.*, **190**, 71–95.

Lorenz, J.C. and **Nadon, G.C.** (2002) Braided-river deposits in a muddy depositional setting: the Molina Member of the Wasatch Formation (Paleogene), west-central Colorado, USA. *J. Sediment. Res.*, **72**(3), 376–385.

Lucas, S.G. and **Tanner, L.H.** (2014) Unconformable contact of the lower Jurassic Wingate and Kayenta Formations, southeastern Utah. In: *Geology of Utah's Far South* (Eds MacLean, J.S., Biek, R.F. and Huntoon, J.E.), *Utah Geological Association Publication*, **43**, 311–320.

Luttrell, P.R. (1993) Basinwide sedimentation and the continuum of paleoflow in an ancient river system: Kayenta Formation (Lower Jurassic), central portion Colorado Plateau. *Sed. Geol.*, **85**(1–4), 411–434.

Mabutt, J.A. (1977) *Desert Landforms*. MIT Press, Cambridge, MA. 340 pp.

Mackey, S.D. and **Bridge, J.S.** (1995) Three-dimensional model of alluvial stratigraphy; theory and applications. *J. Sediment. Res.*, **65**(1b), 7–31.

Mather, A. (2007) Arid Environments. In: *Environmental Sedimentology* (Eds Perry, C. and Taylor, K.), 1st edn., pp. 144-189.Blackwell Publishing, Oxford.

Miall, A.D. (1977) A review of the braided-river depositional environment. *Earth Sci. Rev.*, **13**(1), 1–62.

Miall, A.D. (1988) Architectural elements and bounding surfaces in fluvial deposits: anatomy of the Kayenta Formation (Lower Jurassic), southwest Colorado. *Sed. Geol.*, **55**(3–4), 233–262.

Miall, A.D. (1996) *The Geology of Fluvial Deposits, Sedimentary Facies, Basin Analysis and Petroleum Geology*, 1st edn. Springer-Verlag, Berlin.

Miall, A.D. (2014) The facies and architecture of fluvial systems. In: *Fluvial Depositional Systems* (Ed. Miall, A.D.), 1st edn., pp. 9–68.Springer, Cham.

Middleton, L.T. and **Blakey, R.C.** (1983) Processes and controls on the intertonguing of the Kayenta and Navajo Formations, northern Arizona: eolian-fluvial interactions. In: *Eolian Sediments and Processes* (Eds Brookfield, M.E. and Ahlbrandt, T.S.), *Dev. Sediment.*, **38**, 613-634.

Nanson, G.C. and **Knighton, A.D.** (1996) Anabranching rivers: their cause, character and classification. *Earth Surf. Proc. Land.*, **21**(3), 217–239.

Nichols, G.J. (1987) Structural controls on fluvial distributary systems–the Luna System, Northern Spain. In: *Recent Developments in Fluvial Sedimentology* (Eds Ethridge, F.G., Florez, R.M. and Harvey, M.D.), *SEPM Special Publication*, **39**, 269–277.

Nichols, G.J. (1989) Structural and sedimentological evolution of part of the west central Spanish Pyrenees in the Late Tertiary. *J. Geol. Soc.*, **146**, 851–857.

Nichols, G.J. and **Fisher, J.A.** (2007) Processes, facies and architecture of fluvial distributary system deposits. *Sed. Geol.*, **195**(1–2), 75–90.

Nichols, G.J. and **Hirst, J.P.** (1998) Alluvial fans and fluvial distributary systems, Oligo-Miocene, northern Spain; contrasting processes and products. *J. Sedim. Res.*, **68**(5), 879–889.

North, C.P. and **Taylor, K.S.** (1996) Ephemeral-fluvial deposits: integrated outcrop and simulation studies reveal complexity. *AAPG Bulletin*, **80**(6), 811–830.

North, C.P. and **Warwick, G.L.** (2007) Fluvial fans: myths, misconceptions, and the end of the terminal-fan model. *J. Sediment. Res.*, **77**(9), 693–701.

Owen, A., **Nichols, G.J.**, **Hartley, A.J.**, **Weissmann, G.S.** and **Scuderi, L.A.** (2015) Quantification of a distributive fluvial system: the Salt Wash DFS of the Morrison Formation, SW USA. *J. Sediment. Res.*, **85**(5), 544–561.

Peterson, F. and **Pipiringos, G.N.** (1979) Stratigraphic relations of the Navajo Sandstone to Middle Jurassic formations, southern Utah and northern Arizona. *Prof. Paper. US Geol. Survey*, **1035-B**, 1–43.

Pettigrew, R.P., **Rogers, S.L.** and **Clarke, S.M.** (2019) A microfacies analysis of arid continental carbonates from the Cedar Mesa Sandstone Formation, Utah, USA. *Deposition. Rec.*, **6**(1), 41–61.

Picard, M.D. and **High, L.R.** (1973) Sedimentary Structures of Ephemeral Streams. *Dev. Sedimentol.*, **17**, 223.

Pipiringos, G.N. and **O'Sullivan, R.B.** (1978) *Principal Unconformities in Triassic and Jurassic Rocks, Western Interior United States; A Preliminary Survey (No. 1035-A)*. United States Government Printing Office, Washington, DC.

Priddy, C.L. and **Clarke, S.M.** (2020) The sedimentology of an ephemeral fluvial-aeolian succession. *Sedimentology*, **67**(5), 2392–2425.

Priddy, C.L., **Pringle, J.K.**, **Clarke, S.M.** and **Pettigrew, R.P.** (2019) Application of photogrammetry to generate quantitative geobody data in ephemeral fluvial systems. *Photogram Rec*, **34**(168), 428–444.

Pringle, J.K., **Brunt, R.L.**, **Hodgson, D.M.** and **Flint, S.S.** (2010) Capturing stratigraphic and sedimentological complexity in 3D digital outcrop models of submarine channel complexes, Karoo Basin, South Africa. *Petrol. Geosci.*, **16**(4), 307–330.

Rarity, F., **Van Lanen, X.M.T.**, **Hodgetts, D.**, **Gawthorpe, R.L.**, **Wilson, P.**, **Fabuel-Perez, I.** and **Redfern, J.** (2014) LiDAR-based digital outcrops for sedimentological analysis: workflows and techniques. *Geol. Soc., London, Spec. Public.*, **387**(1), 153–183.

Reis, A.D.D., **Scherer, C.M.D.S.**, **Amarante, F.B.D.**, **Rossetti, M.D.M.M.**, **Kifumbi, C.**, **Souza, E.G.D.**, **Ferronatto, J.P.F.** and **Owen, A.** (2019) Sedimentology of the proximal portion of a large-scale, Upper Jurassic fluvial-aeolian system in Paraná Basin, southwestern Gondwana. *J. S. Am. Earth Sci.*, **95**, 102248.

Riggs, N.R. and **Blakey, R.C.** (1993) Early and Middle Jurassic paleogeography and volcanology of Arizona and adjacent areas. In: *Mesozoic Paleogeography of the Western United States—II: Los Angeles, Pacific Section* (Eds Dunne, G.C. and McDougall, K.C.), *SEPM (Society for Sedimentary Geology)*, **71**, 347–373.

Sambrook Smith, G.H., **Best, J.L.**, **Ashworth, P.J.**, **Fielding, C.R.**, **Goodbred, S.L.** and **Prokocki, E.W.** (2010) Fluvial form in modern continental sedimentary basins: Distributive fluvial systems: COMMENT. *Geology*, **38**(12), 230.

Stanistreet, I.G. and **McCarthy, T.S.** (1993) The Okavango Fan and the classification of subaerial fan systems. *Sed. Geol.*, **85**(1–4), 115–133.

Stear, W.M. (1985) Comparison of the bedform distribution and dynamics of modern and ancient sandy ephemeral flood deposits in the southwestern Karoo region, South Africa. *Sediment. Geol.*, **45**(3–4), 209–230.

Sutfin, N.A., **Shaw, J.R.**, **Wohl, E.E.** and **Cooper, D.J.** (2014) A geomorphic classification of ephemeral channels in a mountainous, arid region, southwestern Arizona, USA. *Geomorphology*, **221**, 164–175.

Terwisscha van Scheltinga, R.C., **McMahon, W.J.**, **van Dijk, W.M.**, **Eggenhuisen, J.T.** and **Kleinhans, M.G.** (2020) Experimental distributive fluvial systems: Bridging the gap between river and rock record. *Deposition. Rec.*, **6**(3), 670–684.

Todd, S.P. (1996) Process deduction from fluvial sedimentary structures. In: *Advances in Fluvial Dynamics and Stratigraphy* (Eds Carling, P.A. and Dawson, M.R.), pp. 299–350.Wiley, West Sussex.

Tooth, S. (2000) Process, form and change in dryland rivers: a review of recent research. *Earth Sci. Rev.*, **51**(1–4), 67–107.

Tooth, S. (2005) Splay formation along the lower reaches of ephemeral rivers on the Northern Plains of arid central Australia. *J. Sediment. Res.*, **75**(4), 636–649.

Tooth, S. and **Nanson, G.C.** (1999) Anabranching rivers on the Northern Plains of arid central Australia. *Geomorphology*, **29**(3–4), 211–233.

Tunbridge, I.P. (1981) Sandy high-energy flood sedimentation—some criteria for recognition, with an example from the Devonian of SW England. *Sed. Geol.*, **28** (2), 79–95.

Tunbridge, I.P. (1984) Facies model for a sandy ephemeral stream and clay playa complex; the Middle Devonian Trentishoe Formation of North Devon, UK. *Sedimentology*, **31**(5), 697–715.

Veiga, G.D., **Spalletti, L.A.** and **Flint, S.** (2002) Aeolian/fluvial interactions and high-resolution sequence stratigraphy of a non-marine lowstand wedge: the Avilé Member of the Agrio Formation (Lower Cretaceous), central Neuquén Basin, Argentina. *Sedimentology*, **49**, 1001–1019.

Ventra, D. and **Clarke, L.E.** (2018) Geology and geomorphology of alluvial and fluvial fans: current progress and research perspectives. *Geol. Soc., London, Spec. Public.*, **440**(1), 1–21.

Visser, C.A. and **Chessa, A.G.** (2000) A new method for estimating lengths for partially exposed features. *Math. Geol.*, **32**(1), 109–126.

Weissmann, G.S., **Hartley, A.J.**, **Nichols, G.J.**, **Scuderi, L.A.**, **Olson, M.**, **Buehler, H.** and **Banteah, R.** (2010) Fluvial form in modern continental sedimentary basins: distributive fluvial systems. *Geology*, **38**(1), 39–42.

Weissmann, G.S., **Hartley, A.J.**, **Scuderi, L.A.**, **Nichols, G.J.**, **Davidson, S.K.**, **Owen, A.**, **Atchley, S.C.**, **Bhattacharyya, P.**, **Chakraborty, T.**, **Ghosh, P.** and **Nordt, L.C.** (2013) Prograding distributive fluvial systems: geomorphic models and ancient examples. In: *New Frontiers in Paleopedology and Terrestrial Paleoclimatology* (Eds Driese, S.G. and Nordt, L.C.), *SEPM, Special Publication*, **104**, 131–147.

Williams, G.P. (1970) Flume width and water depth effects in some sediment-transport experiments. *U.S. Geol. Sur. Prof. Paper*, **562-H**, 37.

Williams, G.E. (1971) Flood deposits of the sand-bed ephemeral streams of central Australia. *Sedimentology*, **17** (1–2), 1–40.

Wilson, R.F. (1958) *The stratigraphy and sedimentology of the (Jurassic) Kayenta and (?Triassic) Moenave Formations, Vermilion Cliffs region, Utah and Arizona*. Unpublished PhD Thesis. Stanford University, Stanford, CA.

Manuscript received 15 June 2020; revision 15 March 2021; revision accepted 24 March 2021